Aquaculture 598 (2025) 741962

Contents lists available at ScienceDirect

Aquaculture

journal homepage: www.elsevier.com/locate/aquaculture

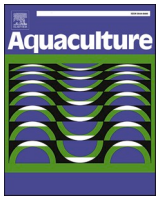

Genetic basis analysis and genome prediction of swimming performance traits in juvenile spotted sea bass (*Lateolabrax maculatus*)

Hao Li [a,1], Chong Zhang [a,1], Haishen Wen [a], Xin Qi [a], Yani Dong [a], Cong Liu [a], Yonghang Zhang [a], Chunxiang Niu [a], Yun Li [a,b,*,2]

[a] Key Laboratory of Mariculture, Ministry of Education (KLMME), Ocean University of China, Qingdao 266003, China
[b] Sanya Oceanographic Institution, Ocean University of China, Sanya 572000, China

ARTICLE INFO

Keywords:
Deeper offshore aquaculture
Lateolabrax maculatus
Swimming performance
GWAS
Genomic selection

ABSTRACT

The swimming performance of fish is crucial for their survival, playing a significant role in enhancing disease resistance and facilitating stress recovery, particularly in aquaculture fish. Understanding the genetic basis of fish swimming performance is essential for its integration as a key trait in selection breeding programs, especially for deeper offshore aquaculture. Spotted sea bass, an economically important aquaculture fish species in China, exhibits euryhaline and eurythermic characteristics and has demonstrated substantial potential for deep-sea aquaculture. Therefore, in our study, the absolute critical swimming speed (a.U_{crit}) of juvenile spotted sea bass were assessed, ranging form 24.50 cm s^{-1} to 65.00 cm s^{-1}, and this range enabled the identification of individuals with superior and inferior swimming abilities within the test population. Based on whole-genome resequencing, genome-wide association studies (GWAS) were conducted for three phenotypes of swimming performance, identifying 25 associated SNPs and 85 candidate genes, indicating that it is a polygenetic trait influenced by multiple biological processes. The heritability estimates for a.U_{crit} and relative critical swimming speed (r.U_{crit}) were 0.21 ± 0.08 and 0.22 ± 0.08, respectively. Furthermore, the impact of various genomic selection (GS) models and SNP densities on prediction accuracy of swimming performance was evaluated using genomic prediction (GP). The SVM model is recommended for continuous trait prediction of swimming performance, especially when SNP densities ranges between 500 and 50 K, as it provides more accurate, efficient and stable predictions. Our research further enhances the understanding of the genetic basis of fish swimming performance and holds promise for improving productivity in deep-sea aquaculture through genomic selection.

1. Introduction

China is the world's largest producer of marine aquaculture, contributing 23.96 million tons in 2023. Conventional nearshore aquaculture methods, including net cages, rafts, and bottom-seeding, account for 66.58 % of the total yield (MOA, 2024). However, the expansion of recreational fishing and tourism has increasingly limited available nearshore aquaculture spaces, and some farming areas are also suffering from water pollution (Mai et al., 2016). These factors significantly hinder the sustainable development of the marine aquaculture industry. In response, China is actively promoting the expansion of mariculture from nearshore to deeper offshore environments (Mai, 2021). Offshore sites present unique challenges, including larger waves and complex hydrological conditions, which place higher demands on the swimming performance and robustness of farmed animals (Zeng et al., 2022). Additionally, suitable species for offshore mariculture in Chinese waters are limited, and the risks associated with farming in open waters remain poorly understood (Peng et al., 2023). This underscores the need to develop and select native species specifically adapted to deep-sea mariculture (McKenzie et al., 2021).

Spotted sea bass (*Lateolabrax maculatus*) is one of the highest-yielding economic mariculture fish species in China. Since 2009, annual production of spotted sea bass in China has consistently surpassed 100,000 tons, and in 2023, the annual yield exceeded 240,000 tons (MOA, 2024), reflecting substantial market demand. Currently, the majority of farmed spotted sea bass in China are cultured in traditional

* Corresponding author at: Key Laboratory of Mariculture, Ministry of Education (KLMME), Ocean University of China, Qingdao 266003, China.
E-mail address: yunli0116@ouc.edu.cn (Y. Li).
[1] These authors contributed equally to this work.
[2] Full postal address: Ocean University of China, No 5 Yushan road, Qingdao 266003, PR China

https://doi.org/10.1016/j.aquaculture.2024.741962
Received 11 September 2024; Received in revised form 18 November 2024; Accepted 27 November 2024
Available online 2 December 2024

ponds and conventional net cages (Wen et al., 2016). In recent years, there have been practices trying to cultivate spotted sea bass in offshore net cages (Shi et al., 2021), indicating its significant potential for deep-sea cage farming.

Swimming performance is a critical mechanism in fish, significantly influencing their predation, evasion, and overall fitness (Handelsman et al., 2010; Oufiero et al., 2011). Extensive research has been conducted globally on various aspects of fish swimming, including speed, behavior, and the external factors that influence their capabilities (Cano-Barbacil et al., 2020; Katopodis et al., 2019; Shadwick and Goldbogen, 2012). To quantify swimming performance, scientists have developed several indices, such as burst swimming speed, endurance (Beamish, 1978) and gait transition speed (Drucker, 1996). Among these, critical swimming speed (U_{crit}), also known as maximum aerobic swimming speed, represents the velocity at the threshold between aerobic and anaerobic swimming (Brett, 1964). Due to its brief duration and high repeatability, U_{crit} has been wildly applied in studies of fish swimming performance (Norin and Clark, 2016; Pang et al., 2021; Plaut, 2001).

Numerous factors affect fish swimming capabilities, including environmental variables such as water temperature (Grimmelpont et al., 2022), dissolved oxygen (Pang et al., 2015), pollutants (Rao et al., 2022), and salinity(Plaut, 2000), as well as intrinsic morphological (Gregory and Wood, 1998) and physiological attributes. Notably, sustained aerobic exercise has been shown to enhance fish resilience, improving growth performance, immune response (Castro et al., 2013; Kolok and Farrell, 1994; McKenzie et al., 2021), and cardiac function (Claireaux et al., 2005). Additionally, swimming facilitates the recovery of fish from acute stressors, including live transport (Arbeláez-Rojas et al., 2017), confinement (McKenzie et al., 2012), and handling (Young and Cech, 1993). For example, swimming endurance of Atlantic salmon (*Salmo salar*) has been significantly correlated with disease resistance, with faster swimmers exhibiting enhanced immunity (Castro et al., 2013). Several studies have explored swimming performance as a sub-lethal selection tool for traits such as susceptibility, growth rate, feed intake, and yield in farmed fish (Kolok, 2001; Palstra et al., 2020). While research has indicated that fish swimming performance is a heritable trait, with moderate to high heritability estimated across different species (Garenc et al., 1998; Mengistu et al., 2021), efforts to dissect the genetic basis of swimming performance remain in their early stages. Furthermore, research regarding the swimming abilities of spotted sea bass is limited. Given the crucial role of swimming performance in determining fish adaptability and survival, incorporating this trait into genetic breeding programs of spotted sea bass has significant implications.

To elucidate the genetic basis of swimming performance traits in spotted sea bass and to breed strains more suitable for deeper offshore farming, genome-wide association studies (GWAS) were employed to identify single nucleotide polymorphisms (SNPs) and candidate genes related to these traits. Concurrently, genomic prediction (GP) analyses were conducted to assess prediction accuracy and determine the optimal GS model, along with the most effective SNP density for estimating genomic breeding values (GEBVs) related to swimming performance in spotted sea bass. This research provides theoretical support for understanding the genetic basis of swimming performance in spotted sea bass and for breeding strains adapted to offshore farming.

2. Materials and methods

2.1. Experimental fish and ethics statement

A total of 770 spotted sea bass juveniles used in this study were 7.33 ± 0.54 cm (mean ± SD) in body length (BL), 5.97 ± 1.33 g in body weight (BW), and obtained from Yantai Jinghai Marine Fishery Co., Ltd. (Yantai, China). The fish were acclimated at a recirculating water system of Ocean University of China (Qingdao, China) for two weeks prior to swimming performance test. Water temperature was maintained at around 18 °C, and water dissolved oxygen saturation was kept >80 % with a constant 12 h light/12 h dark cycle. During the acclimation, the salinity of water was decreased from 30 ppt to 0 ppt (around 10 ppt per day) by adding fresh water. The fish were fed twice a day on commercial floating pellet (Xingchang Aquatic technology, China), but were fasted for 48 h prior to the test.

All the animal specimens and experimental procedures were approved by the Animal Research and Ethics Committees of Ocean University of China (Permit Number: 20141201). There were no endangered or protected species included in the present study.

2.2. Swim flume and calibration

The swimming performance of fish were tested at a large flow-controlled recirculating flume at Fisheries College of Ocean University of China, Shandong, China. The test area of the flume measured 4.00 m × 1.00 m × 1.20 m, and a stable flow range of 0.2 to 0.7 m s^{-1} can be provided. To simulate the effect of water flow on fish in a marine aquaculture environment, a net cage (1.00 m × 0.50 m × 0.25 m) was set up in the flume, and experimental fish are placed in the net cage for experimentation (Fig. 1A). To prevent fish from jumping out of the net cage, the water depth inside the cage was 15 cm with 10 cm of outlet height.

To calibrate the swim tunnel, a flow meter (XIANGRUIDE LS300-A, China) was used to take point velocity measurements in 3 points of each four cross-sections of swim tunnel (Fig. 1B, C). Based on the calibration result, the deference of flow rates among different points within the net cage maintained at a low level (± 1 cm s^{-1}, SD), ensuring that the swimming of test fish was not influenced by their distribution in the net cage.

2.3. Swimming performance test

A total of 770 spotted sea bass were subjected to swimming performance tests. Critical swimming speed (U_{crit}) were tested to quantify the swimming performance of fish by using Ramp-U_{crit} test method with some adjustments (Farrell, 2008). And before formal experiments, a prior practice swim test was performed to obtain a more scientifically sound flow rate increment program. Each time, 70 fish were selected randomly and introduced into the net cage, and the water velocity in the flume was adjusted by changing the engine rotation frequency.

Initially, the water velocity inside the net cage was set at 10 cm s^{-1} (around 1 BL s^{-1}) and maintained for 30 min to allow the experimental fish recover from the stress of being transferred. Subsequently, with water velocity increment of 5 cm s^{-1} and time steps of 5 min to rapidly increase the flow rate inside the net cage to half of the mean absolute swimming speed (a.U_{crit}) (25 cm s^{-1}, determined based on the preliminary experiment). Then, the water velocity was gradually increased in increments of 10 cm s^{-1} with time steps of 15 min (as shown in the Fig. 1D) until the experimental fish were fatigued. Fatigue was determined when the fish could not swim away from the back net of the cage, even when physically stimulated. The exhaustion time was immediately recorded, the fish was removed from the net cage, weighed, photographed, and a fin clip was sampled and preserved for DNA extraction. The experiment ended when all the experimental fish in the net cage reached exhaustion. The a.U_{crit} of the experimental fish was calculated using the following formula:

$$a.U_{crit} = U1 + (T1/T2) \times U2$$

where $U1$ is the highest water velocity that an individual can swim for the entire time period, $U2$ is the water velocity at which an individual fatigued, T1 is the time an individual managed to swim at $U2$, T2 is the time increment of $U2$.

And the relative critical swimming speed (r.U_{crit}) was calculated using the formula:

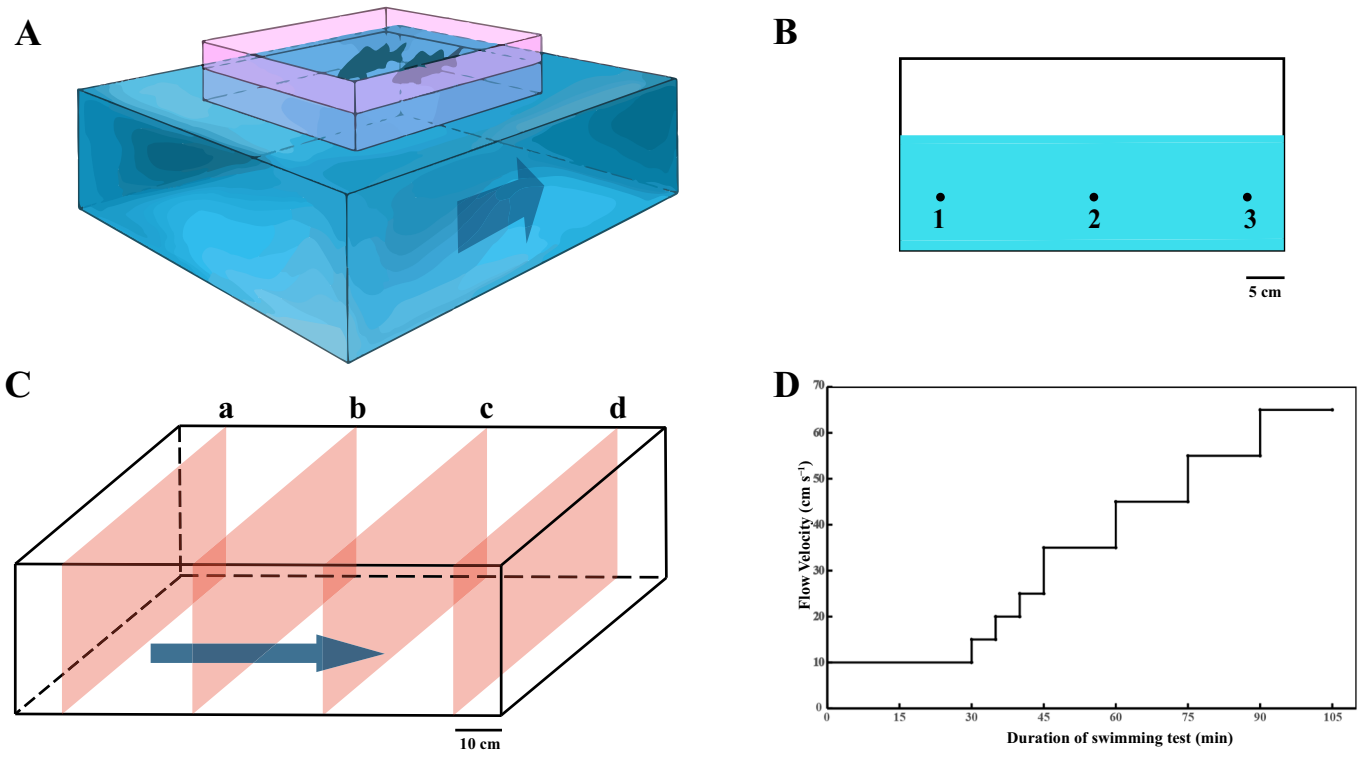

Fig. 1. The swim tunnel and the flow change during swimming performance test. (A) Diagram of the test region of the swim tunnel (blue cube) and the net cage (pink area). The dark blue arrow represents the flow direction. (B) Three points (1, 2 and 3) measured for water flow velocity at each cross section inside the net cage, and the blue area represents the water height. (C) Diagram of the net cage and four cross sections (red parallelograms a, b, c, and d) for velocity measurement points. (D) A schematic representation of the incremental changes in water velocity. (For interpretation of the references to color in this figure legend, the reader is referred to the web version of this article.)

$$r.U_{crit} = a.U_{crit}/BL$$

where BL is the body length of the tested fish.

All tests were carried out at a water temperature of around 14 °C and oxygen content of ≥90 % saturation. After all the swimming tests were completed, fish with a.U_{crit} ranking top 30 % and last lowest 30 % in the test population were further classified as superior swimmers (SS) and inferior swimmers (IS), respectively.

2.4. DNA extraction, library construction and sequencing

Caudal fin samples of 446 spotted sea bass (228 SS and 218 IS) were used to extract DNA by using TIANamp Marine Animals DNA Kit (Tiangen, China). DNA integrity and concentration were assessed based on 1 % agarose gel electrophoresis and Qubit Flex Fluorometer (ThermoFisher, USA). DNA library preparation was performed by using VAHTs Universal Plus DNA Library Prep Kit for Illumina (Vazyme, China) according to the protocols from manufacturer. Each library was sequenced using Illumina NovaSeq X plus platform to generate 150 bp pair-end (PE) reads at Novogene Technology Co., Ltd. (Beijing, China).

2.5. Genotyping and quality control

The raw reads were obtained and filtered using SOAPnuke (v2.0) to remove the paired reads that contained the adapters, reads that possessed N bases (ambiguous bases) > 10 % of the total read length and reads with low quality (Q ≤ 5) bases >50 % of the total read length (Chen et al., 2017). After the filtering, clean reads were aligned to the reference genome of spotted sea bass (JAYMHB000000000) using bwa (v0.7.17) with default arguments. The Genome Analysis toolkit (GATK) (v4.1.3.0) was used to conduct variants calling and hard filtering (Van der Auwera and O'Connor, 2020). For the hard filtering, variants were kept with the thresholds set as depth/variant confidence (QD) ≥ 2.0, fisher strand (FS) ≤ 60.0, RMS mapping quality (MQ) ≥ 40.0, MQRankSum ≥ −12.5, ReadPosRankSum ≥ −8.0 and StrandOddsRatio (SOR) > 3.0. PLINK (v1.90) was used to perform genotype quality control, remove the SNPs with (1) minor allele frequency (−maf) < 0.05; (2) SNPs with missing rate (−geno) > 0.02; (3) Hardy-Weinberg equilibrium FDR *P*-value (−hwe) < 1e-4; and individuals with (4) variant missing rate (−mind) > 0.05. After the quality control, the missing genotypes were imputed with Beagle (v5.2). The distribution of SNPs in different chromosomes of spotted sea bass was visualized by CMplot R package.

2.6. Linkage disequilibrium (LD) and population structure analysis

By using the PopLDdecay (v3.42) software, the LD coefficient (r^2) between two SNPs was calculated and the genome-wide pattern of LD decay plot was drawn (Zhang et al., 2019). Principle component analysis (PCA) was implemented using PLINK (v1.90) to display the population components. The maximum likelihood model of Admixture (v1.3.0) software (Alexander et al., 2009) was used to calculate population structure, and the K-value (the putative number of genetic group) was set to 1–10. Additionally, to get better understanding of the relatedness of individuals, a kinship analysis was performed with Tassel (v5.0). The PCA plot and kinship heat map were drawn with ggplot2 R package and pheatmap, respectively.

2.7. Genome-wide association study (GWAS)

Three phenotypes of swimming performance were used to analyze: (1) the absolute critical swimming speed (a.U_{crit}); (2) the relative critical swimming speed (r.U_{crit}); and (3) the binary trait (the SS and IS individuals, recorded as 1 and 2, respectively). GWAS of the a.U_{crit} or r.

U_{crit} and SNPs were performed using the Linear Mixed Model (LMM) of GEMMA (v0.98.5) (Zhou and Stephens, 2012). And GWAS of the binary trait and SNPs was performed using logistic model of PLINK (v1.90). The calculation model is as follow:

$$y = W\alpha + X\beta + Z\mu + \varepsilon$$

where y is the swimming performance trait of individuals; W is the matrix of covariates (fixed effects), α is vector of corresponding coefficients including the first three principal components and BL (for r.U_{crit} and binary trait); X is the matrix of marker genotypes (fixed effect); β is the allele substitution effect of each SNP; Z is the genomic kinship matrix based on SNPs, μ is the additive genetic effect; and ε is the vector of residual errors.

Given that the initially set Bonferroni-corrected significance association threshold was considered too stringent and prone to false negatives, PLINK (v1.90) was used to conduct LD pruning and count the number of tag SNPs (N), representative SNPs in the haplotype region of the genome. Therefore, 0.05/N and 1/N were set as the final genome-wide significance association threshold and the suggestive association threshold, respectively. The Manhattan plots and QQ-plots were drawn by CMplot package in RStudio. And the phenotypic variance explained (PVE) of swimming performance traits was estimated based on the GEMMA (v0.98.5) result files and according to the formula mentioned in article by Heejung Shim et al. (Shim et al., 2015).

The detailed information of significant associated SNPs were annotated by using snpEff (v5.2–0) (Cingolani et al., 2012). The candidate genes were scanned ±50 kb surrounding the SNPs in reference genome of spotted sea bass using bedtools (v2.31.0), and were ensured by BLAST against the non-redundant protein database. Gene Ontology (GO) enrichment analysis of the candidate genes was performed by using KOBAS website (http://bioinfo.org/kobas/genelist/).

2.8. Genomic prediction (GP)

The narrow-sense heritability (h^2) of swimming performance of spotted sea bass was estimated using GCTA (v1.94.0). Variance components were estimated using GREML (genome-based restricted maximum likelihood), and the heritability of two traits (a.U_{crit} and r.U_{crit}) were determined using the formula: $h^2 = \sigma_g^2/(\sigma_g^2 + \sigma_e^2)$, where σ_g^2 is the additive genetic variance contributed by all SNPs and σ_e^2 is the residual variance (Yang et al., 2011).

To assess the feasibility of genomic selection (GS) for improving the swimming performance in spotted sea bass, genomic prediction (GP) was conducted to evaluate the predictive accuracies of both r.U_{crit} and binary trait (i.e., IS and SS). To mitigate the multicollinearity of GS model caused by adjacent SNPs that highly correlated with each other, the tag SNPs were selected for the subsequent GP analyses. The prediction accuracies of various SNP panels (10, 25, 50, 75, 100, 200, 500, 1 K, 5 K, 10 K, 20 K, 50 K, 100 K, and All SNPs) were compared across eight GS models. The GS models used herein included six traditional models (rrBLUP (Ridge Regression Best Linear Unbiased Prediction), BayesA, BayesB, BayesC, Bayesian Lasso (BayesL) and BayesRR (Bayesian Ridge Regression)) and two machine learning models (RKHS (Reproducing Kernel Hilbert Space) and SVM (Support Vector Machine)).

The traditional models could be generalized as:

$$y = Xb + Zg + e$$

where y is the vector of phenotypic values; b is the vector of fixed effect including the first three principal components; g is the vector of additive genetic values (SNPs effect); e is the vector of residual effect; X and Z are incidence matrices relating the fixed effect and additive genetic values. RKHS and SVM are kernel-based algorithms (Nayeri et al., 2019). RKHS substitutes the genomic relationship matrix with a general kernel matrix, which allows for the assessment of similarities among individuals, even in the absence of genetic correlation (González-Recio et al., 2014). SVM, initially designed as a classifier, was created to separate hyperplanes that maximize the geometric margin, effectively ensuring accurate division of a specified training dataset (Howard et al., 2014).

rrBLUP model was performed using R package rrBLUP (v4.6.3), SVM model was performed using R package Kernlab (v0.9–32) (kernel = "rbfdot", epsilon = 0.01, C = 1), and the other five Bayesian and RKHS models were operated using R package BGLR (v1.1.2) (nIter = the number of SNPs (when the number of SNPs ≤ 1000, nIter = 1000), burnIn = 1/10 nIter, df0 = 5, and h = 0.1 for RKHS) (Endelman, 2011; Karatzoglou et al., 2004; Perez and de los Campos, 2014). 10 % of the samples were selected randomly as testing population, while the remaining 90 % served as training population and were used for GWAS analyses. The SNPs with lowest ranked *P*-value based on the result of GWAS were selected for each SNP panel. The prediction ability of each model were represented by two metrics: the Pearson correlation coefficient (PCC) between the observed phenotypes and genomic estimated breeding value (GEBV) of testing population, and area under the curve (AUC) by 30 replicates of ten-fold cross-validation analyses. The data was then analyzed using IBM SPSS Statistic (v25) and graphed using R studio (v2023.09.1) software, respectively.

3. Results

3.1. The swimming performance of juvenile spotted sea bass

A total of 770 spotted sea bass juveniles were subjected to swimming performance tests. The a.U_{crit} and r.U_{crit} of test population showed approximately normal distribution (Fig. 2). The a.U_{crit} of juvenile spotted sea bass ranged form 24.50 cm s^{-1} to 65.00 cm s^{-1}, averaging 41.80 ± 7.50 cm s^{-1} (mean ± SD). The r.U_{crit} of juvenile spotted sea bass ranged from 2.95 BL s^{-1} to 8.00 BL s^{-1}, averaging 5.71 ± 0.92 BL s^{-1} (Table 1).

Based on the a.U_{crit}, individuals ranking top 30 % were classified as the superior swimmers (SS) group, and last lowest 30 % in the test population were classified as inferior swimmers (IS) group. Significant differences were observed between the IS group and SS groups in terms of both a.U_{crit} (33.50 ± 4.27 cm s^{-1} vs. 50.15 ± 4.08 cm s^{-1}; *t*-test, $P < 0.0001$) and r.U_{crit} (4.71 ± 0.69 BL s^{-1} vs. 6.57 ± 0.51 BL s^{-1}; *t*-test, $P < 0.0001$) (Fig. 3). In addition, the body length and body weight between SS group and IS group differed significantly (*t*-test, $P < 0.0001$) (Fig. 3), and these were consequently included as covariates for subsequent GWAS analyses.

3.2. Genotyping results and marker distribution

A total of 446 caudal fin samples of juvenile spotted sea bass were used for DNA extraction, library construction and sequencing, and 11 samples were discarded due to quality control. After quality control, 2,124,413 high-quality SNPs were obtained and used for further analyses. Of those, 1,742,824 (61.83 %) SNPs were located in the intergenic regions, while 1,129,098 (35.94 %) SNPs were located in gene coding sequence. Among the SNPs in coding regions, 124,619 (3.966 %) were situated in the exon region, and the ratio of nonsynonymous SNPs to synonymous SNPs was 1:1.76 (43,592/76,844). The total physical distance covered by these SNPs was 607.02 Mb, and these SNPs are densely and evenly distributed in the genome with the average density of SNP/292 bp (Fig. 4A).

3.3. Population structure and kinship analysis

LD analysis showed a rapid declining trend with squared correlation coefficient (r^2) between two loci decreased rapidly to 0.1 when the distance between each pair of SNPs was around 150 bp (Fig. 4B). To assess the population structure of sequenced individuals, principal

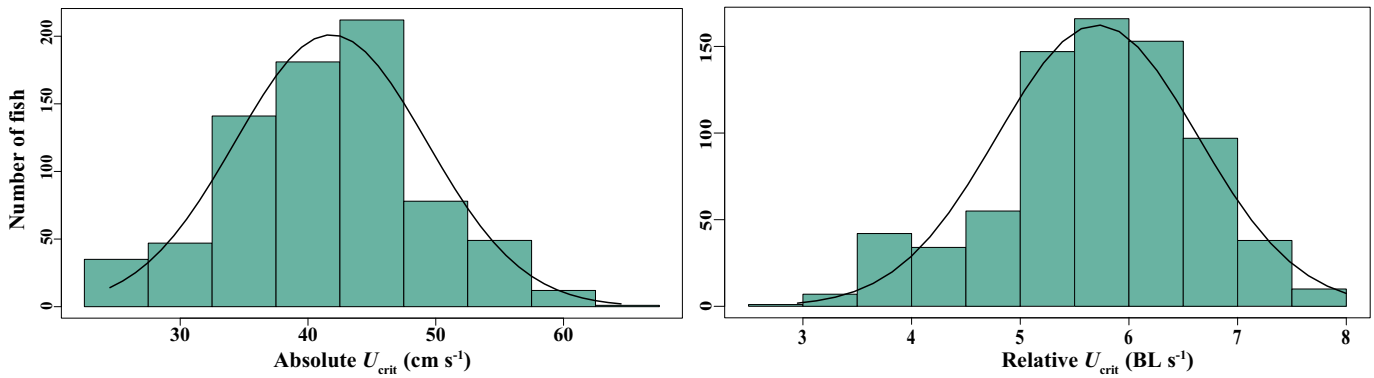

Fig. 2. The distribution of swimming performance of juvenile spotted sea bass. Solid black curves fitting normal distributions based on the given a.U_{crit} and r.U_{crit} are presented.

Table 1
Number of fish (N), body length (BL, mean ± SD), body weight (BW), absolute critical swimming speed (a.U_{crit}) and relative critical swimming speed (r.U_{crit}) of juveniles of spotted sea bass.

	N	BL/cm	BW/g	a.U_{crit}/ cm·s^{-1}	r.U_{cirt}/ BL·s^{-1}
All Sample	770	7.32 ± 0.56	5.97 ± 1.33	41.80 ± 7.50	5.71 ± 0.92
IS Group	218	7.15 ± 0.53	5.56 ± 1.26	33.50 ± 4.26	4.71 ± 0.69
SS Group	228	7.64 ± 0.50	6.70 ± 1.35	50.15 ± 4.08	6.57 ± 0.51

IS, inferior swimmers; SS superior swimmers.

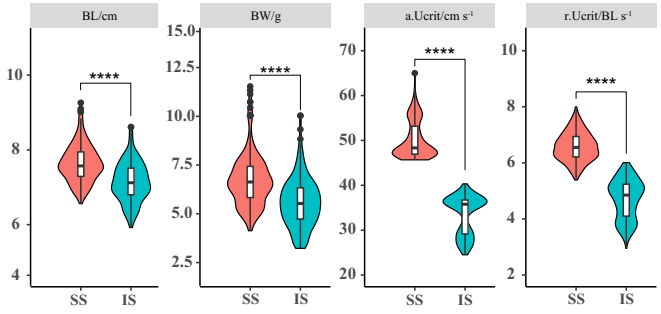

Fig. 3. The body length (BL), body weight (BW), absolute critical swimming speed (a.U_{crit}) and relative critical swimming speed (r.U_{crit}) of spotted sea bass with different swimming performance. SS, superior swimmers group, and IS, inferior swimmers group.

component analysis (PCA) and kinship matrix were employed. The PCA showed that 435 spotted sea bass populations clustered into several discrete subgroups, while individuals of the IS and SS groups were generally evenly distributed. The PC1 and PC2, explained 38.30 % and 19.19 % of the total variance, respectively (Fig. 4C). A three-dimensional principal component analysis (PCA) plot were also provided in supplementary Fig. S1 to better illustrate the relationships between samples. Additionally, population structure analysis showed that the cross-validation (CV) value reached the minimum at a K-value of 9 (Fig. S2), indicating the optimal number of genetic group for testing population (Fig. 4D). The heatmap of kinship relatedness matrix demonstrated that the genetic kinship of these individuals was weak, due to the most genetic relatedness values were very low (Fig. 5). Consequently, the kinship matrix was added to the GWAS model as a random effects covariable matrix.

3.4. GWAS of swimming performance traits

Three types of swimming performance trait were analyzed using GWAS, including two continuous trait: a.U_{crit} and r.U_{crit}, and one binary trait. A total of 204,235 haplotype blocks for SNPs were identified and and its number was used to set thresholds, respectively (genome-wide significant *P*-value = 2.45e-7, suggestive significant *P*-value = 4.90e-6). For a.U_{crit}, 5 significant and 31 suggestive SNPs were detected (Fig. 6A). For r.U_{crit}, 3 significant and 30 suggestive SNPs were found (Fig. 6B). And for binary trait, 12 suggestive SNPs were identified (Fig. 6C). By selecting the loci detected by more than 2 traits, 25 SNPs were retained for further research. Among these SNPs, 7 were predominantly located on Chr13, while the remaining SNPs were distributed across Chr1 (5), Chr4 (1), Chr7 (4), Chr17 (2), Chr19 (1), Chr20 (1), Chr23 (1) and Chr24 (3) (Table 2). In addition, these 25 SNPs were identified as significant or suggestive SNPs in both GWAS results of a.U_{crit} and r.U_{crit} (Table 2). Of which, the locus 7_13,642,433, 13_9,399,249 and 20_19,316,641 were significantly associated with a.U_{crit} and r.U_{crit}, while loci 1_32,051,080 and 13_8,265,662 was significantly correlated with a.U_{crit} only. Notably, loci 24_3,585,432 and 24_3,601,736 were identified as significant or suggestive SNPs across three traits, indicating that these two loci were important potential candidate SNP markers.

3.5. Identification of candidate genes

Among the 25 SNPs associated with swimming performance, 16 were located within gene coding sequences, while the remaining 9 SNPs were found in the upstream/downstream (within 5 kb) or intergenic regions. By scanning the 50 kb genome sequences surrounding these significant SNPs, a total of 85 candidate genes were identified (Table S1). Of which, there were 28 candidate genes annotated on Chr 13, including NAD kinase b (*nadkb*), neuronal differentiation 6b (*neurod6b*),insulin-like growth factor-binding protein 1 (*igfbp1*), pH domain and leucine rich repeat protein phosphatase 1 (*phlpp1*). On Chr 7, 25 candidate genes associated with swimming performance were identified, such as cardiotrophin-like cytokine factor 1 (*clcf1*), solute carrier family 43 member 3b (*slc43a3b*) and Smoothelin-like (*smtn*). In addition, the following genes were identified on Chr 1: matrix metallopeptidase 2 (*mmp2*), lysophosphatidylcholine acyltransferase 2 (*lpcat2*), solute carrier family 6 member 2 (*slc6a2*), stathmin-like 4 (*stmn4l*), interleukin 17a (*il17a*) and membrane progestin receptor beta-like (*paqr8l*). The candidate gene inositol 1,4,5-trisphosphate receptor, type 2 (*itpr2*) was identified near locus 4_16319893. Furthermore, cadherin 6-like (*cdh6l*) was recognized as putative candidate gene around 20_19316641. Candidate genes solute carrier family 1 member 1 (*slc1a1*), RAP1, GTP-GDP dissociation stimulator 1 (*rap1gds1*) were identified around 23_3068967, while protein kinase X-linked (*prkx*) and bone morphogenetic protein receptor 2-like (*bmpr2l*) were identified in the intron regions of loci 24_2770096 and 24_3601736, respectively. The gene names and annotations of all these candidate genes were presented in Table S1.

According to GO enrichment analysis, the top 10 GO terms in three

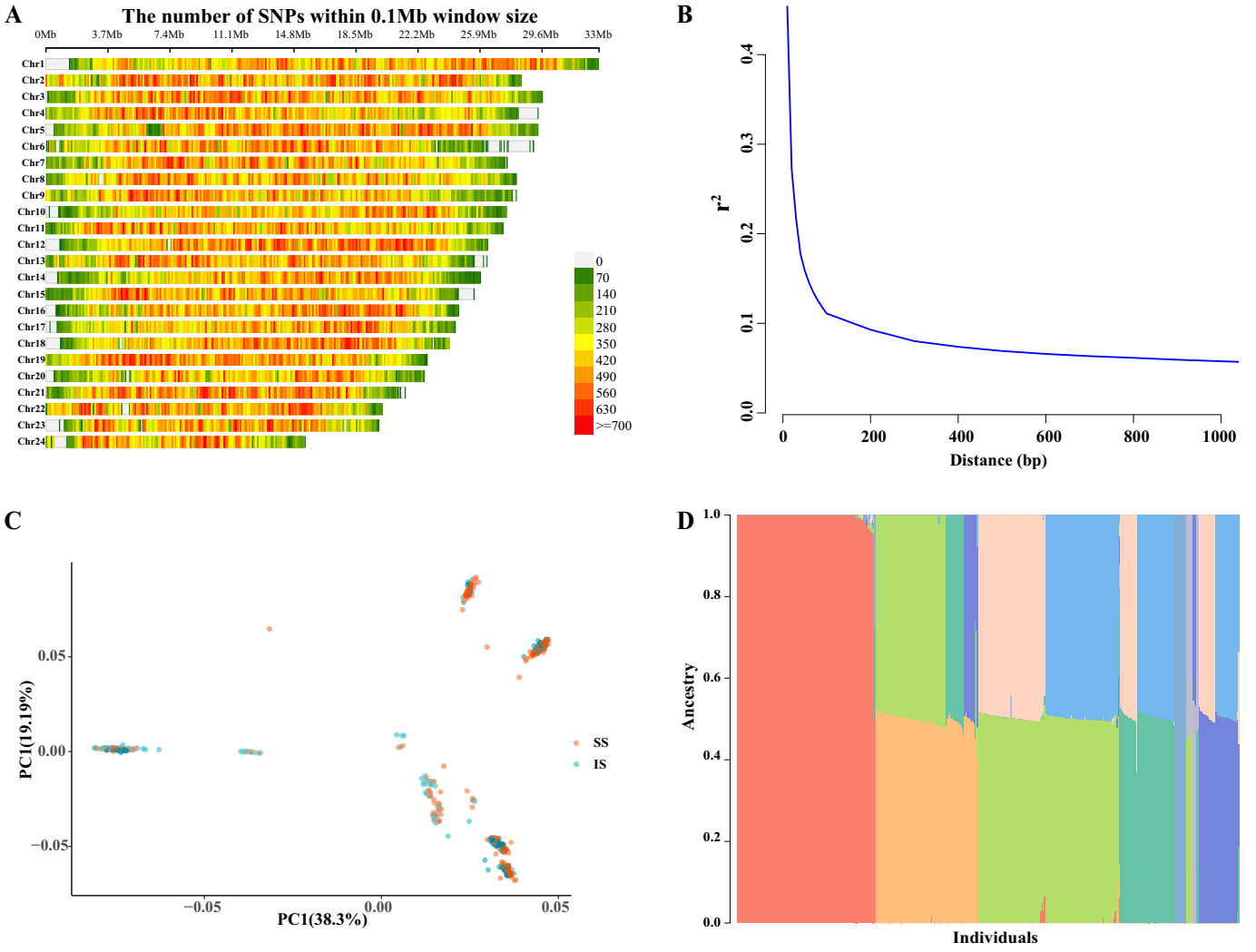

Fig. 4. SNP marker distribution and population structure analyses. (A) SNPs distribution pattern in different chromosomes of spotted sea bass. Different colors represent the corresponding number of SNPs within 0.1 Mb distance according to the legend. (B) LD decay plot of SNPs of spotted sea bass. (C) PCA plot of all individuals based on PC1 and PC2. SS, superior swimmers, and IS, inferior swimmers. (D) The population structure of 435 individuals when K = 9.

main categories (BP, CC and MF) by *P*-value showed that these genes were primarily enriched in signal transduction, development processes and cellular metabolism and function (Fig. 7). Notably, terms such as "cAMP-dependent protein kinase activity" and "calcium ion binding" may influence muscle contraction and neural signal transmission during fish swimming, while terms like "lipid droplet", and "1-acylglycerol-3-phosphate O-acyltransferase activity" may impact the energy supply during swimming (Fig. 7). The potential functional mechanisms of these candidate genes are further described in the "Discussion" section.

3.6. Genomic prediction of swimming performance traits

The estimated heritabilities of a.U_{crit} and r.U_{crit} in spotted sea bass were 0.21 ± 0.08 and 0.22 ± 0.08 (mean ± S.E.), respectively (Table 3). Using PLINK, a total of 204,235 tag SNPs were retained for GP analyses. To assess the feasibility of using genomic selection to improve the offspring swimming performance, we compared the prediction abilities of eight GS models utilizing different SNP panels. In general, the predictive accuracy, assessed through Pearson correlation coefficient (PCC), of r.U_{crit} using different models increased progressively with the number of SNP markers, plateauing around 0.36 at 500 SNPs (Fig. 8A). Specifically, for the Bayesian models, the PCC peaked at 10 K–20 K SNPs (BayesA, 0.38; BayesB, 0.38; BayesC, 0.38; BayesL, 0.39; and BayesRR, 0.38), and then decreased as the number of SNPs increased. Similar to Bayesian models, the PCC of the rrBLUP and RKHS models reached their first peak at 20 K SNPs (0.37 and 0.36, respectively), and then rose to their highest values when using the all SNP panel (rrBLUP, 0.38; and RKHS, 0.43). The PCC of SVM model exhibited an increasing trend with the number of SNPs and reached the highest prediction accuracy of 0.42 with all SNPs. And it provide relatively higher and more stable prediction accuracy when the number of SNPs exceeded 500 compared to other models (Fig. 8A).

For the binary trait, the PCC of the eight GS models displayed trends similar to those for r.U_{crit}, but plateaued around 0.33 at 1 K SNPs (Fig. 8C), indicating that more SNPs were necessary for the binary trait to achieve comparable prediction accuracy. To assess the classification accuracy of each model and trait type, AUC was also calculated. The AUC increased with the number of SNPs, following a trend similar to that of the PCC, regardless of whether it pertained to the continuous trait (r.U_{crit}) or the binary trait (Fig. 8B, D). Although the AUC between r.U_{crit} and binary trait showed no significant difference among different models (Fig. S3), a slightly higher PCC for r.U_{crit} was observed in the comparisons (Fig. S4). In addition, the computational time required by each model varied significantly (Fig. S5). The Bayesian models exhibited similar computational time requirements, which were considerably higher than those for rrBLUP, SVM and RKHS (Fig. S5).

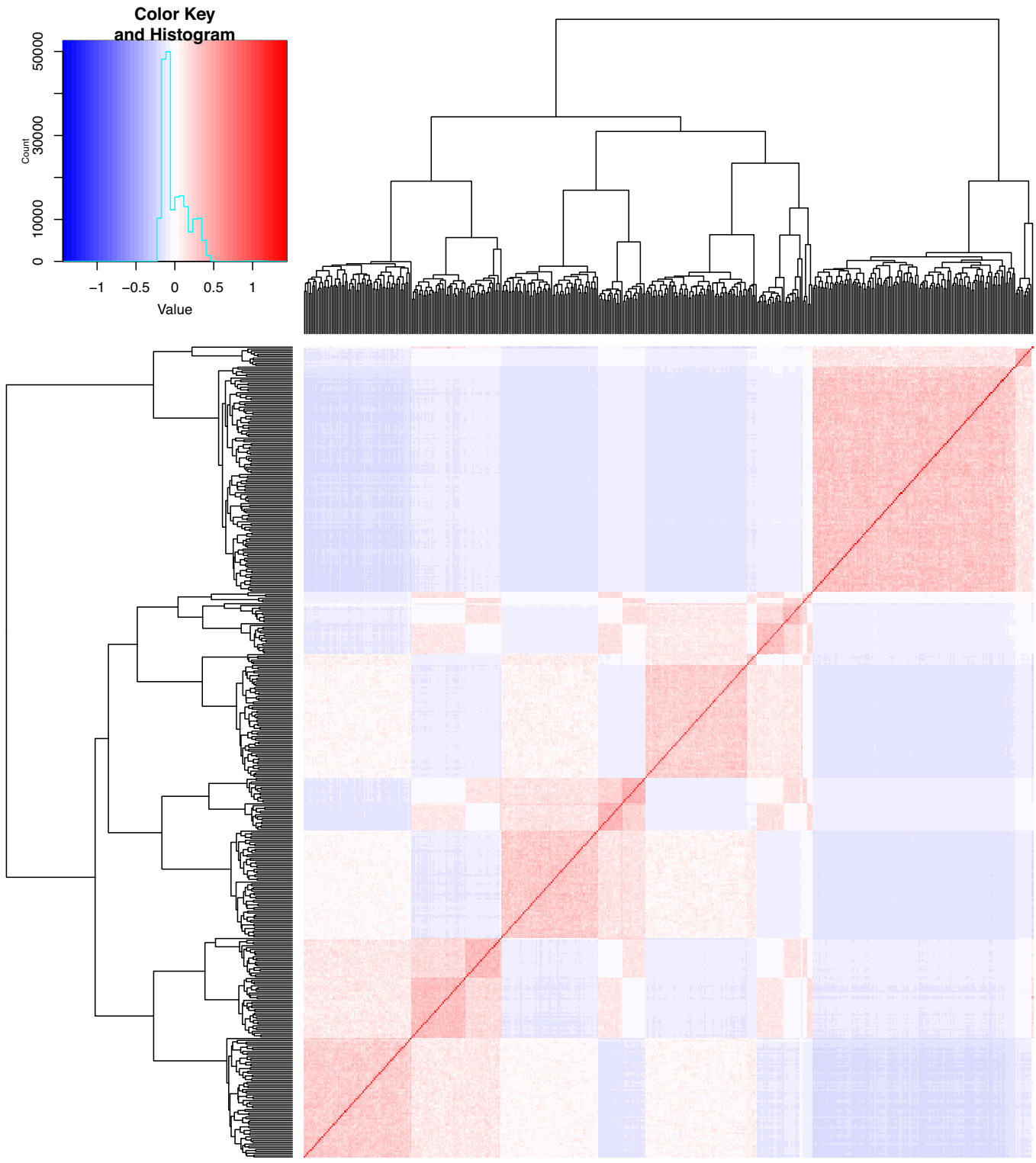

Fig. 5. Kinship among the 435 spotted sea bass samples.

4. Discussion

4.1. The significant difference of swimming performance among spotted sea bass individuals

Ramp-U_{crit} tests were conducted to quantify the swimming performance of spotted sea bass (Farrell, 2008; Jain et al., 1997). Spotted sea bass were farmed in groups within cages, regardless of whether they were in nearshore or offshore mariculture settings. To simulate the conditions of fish farming in cages, a frame cage was constructed and placed in a swim flume, employing a group screening strategy with around 70 fish for each test. Importantly, as the cross-section area of all test fish was smaller than 10 % of the cross-section area of frame cage, the influence of the solid block effect on the measurement of U_{crit} was minimal, and no additional correction was needed (Kern et al., 2018).

The average a.U_{crit} of juvenile spotted sea bass was 41.80 ± 7.50 cm

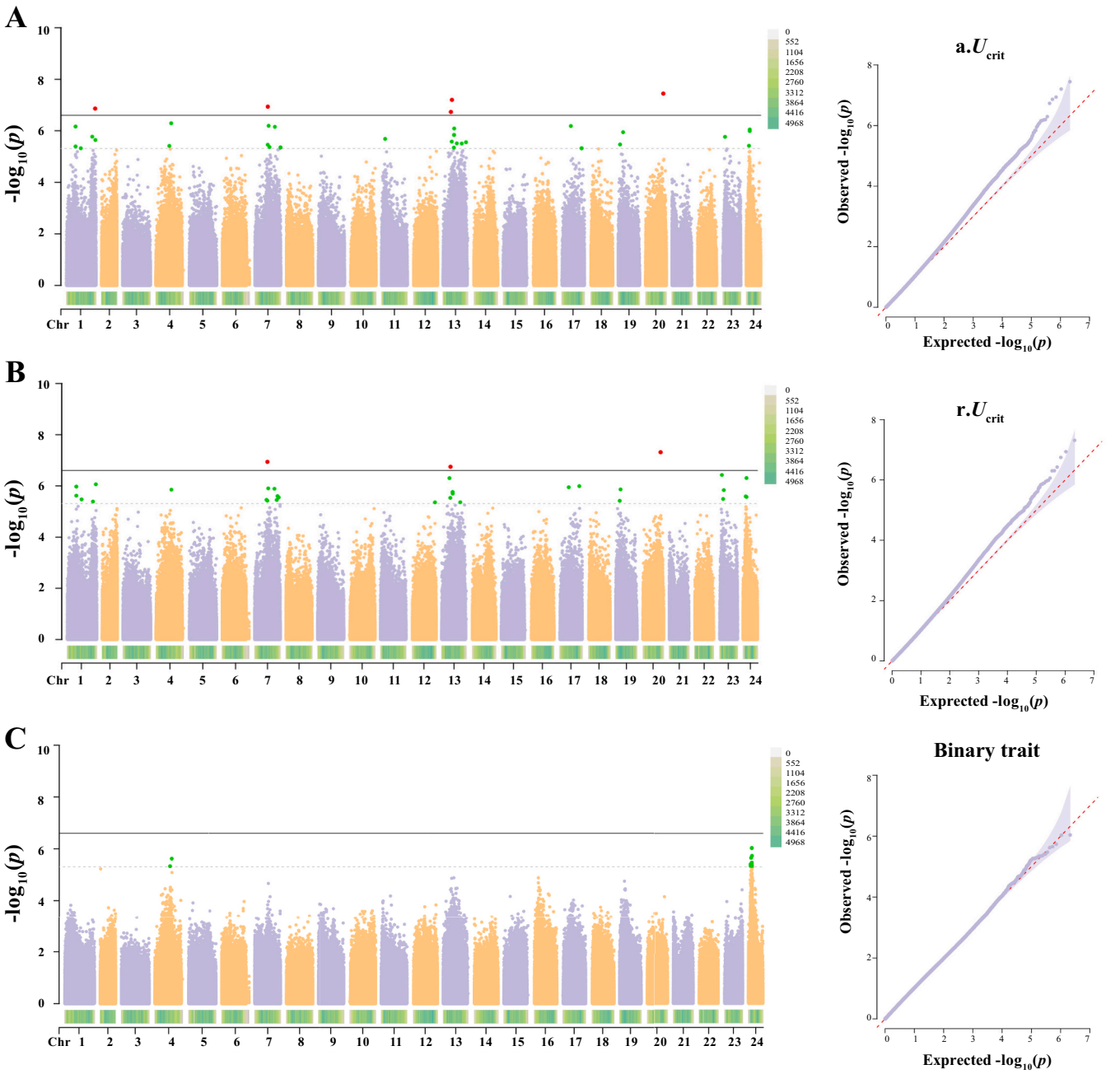

Fig. 6. Manhattan plots (left) and Quantile-Quantile (Q-Q) plots (right) of swimming performance traits in GWAS analysis. (A) GWAS for absolute critical swimming speed (a.U_{crit}). (B) GWAS for relative critical swimming speed (r.U_{crit}). (C) GWAS for binary trait that was classified by a.U_{crit}. In Manhattan plots, the solid lines indicate the *P*-value threshold for genome-wide significance association and the dashed lines indicate the *P*-value threshold for suggestive association.

s^{-1} (mean ± SD), ranging form 24.50 cm s^{-1} to 65.00 cm s^{-1}. Nowadays, in China, native species including the large yellow croaker (*Larimichthys crocea*), spotted sea bass, golden pompano (*Trachinotus ovatus*) and the black rockfish (*Sebastes schlegeli*), have increasingly been utilized for offshore mariculture (Shi et al., 2021). Although there are limited swimming performance measurements available for these farmed fish species with comparable body lengths, the swimming performance of spotted sea bass is considered relative strong (Jing et al., 2005; Wang et al., 2010).

The test population was categorized into superior swimmers (SS) and inferior swimmers (IS) groups based on a.U_{crit}. Previous research in other species has reported a positive correlation between body length, body weight and swimming performance (Cano-Barbacil et al., 2020; Li et al., 2023; Tan et al., 2021). Similarly, the BW and BL of the SS and IS groups also showed a positive correlation with a.U_{crit}. Therefore, it is seemingly possible that selecting for larger body size could lead to obtaining individuals with higher swimming performance. However, it is important to note that performance is influenced by a variety of factors beyond mere size. For instance, significant differences in swimming ability persist even when accounting for size-related factors (as shown by the distribution of r.U_{crit} in Fig. 2B), reflecting the existence of genetic variation (Hanson et al., 2007). Additionally, fish with superior swimming performance may also exhibit enhanced disease resistance and stress recovery capabilities that are genetically determined (Arbeláez-Rojas et al., 2017; Castro et al., 2013). Exclusively selecting for larger body size could overlook these important genetic factors that contribute to robustness. Furthermore, issues may arise in the breeding process when continuously selecting for growth traits, such as degraded

Table 2
The summary of identified SNPs and representative candidate genes associated with swimming performance traits.

SNP_ID	Chr	Position	Allele	MAF	PVE (%)	*P*-value for p1	*P*-value for p2	*P*-value for p3	Location	Candidate Genes
1_11069355	1	11069355	A/C	0.299	0.0248	6.85E-07	1.07E-06		intron	slc6a2
1_11072385	1	11072385	C/A	0.178	0.0213	4.06E-06	2.41E-06		intron	
1_16712163	1	16712163	T/A	0.228	0.0210	4.79E-06	3.37E-06		intergenic	cdyl2
1_28932685	1	28932685	A/G	0.132	0.0230	1.69E-06	4.09E-06		intergenic	
1_32051080	1	32051080	A/G	0.123	0.0279	1.37E-07*	8.68E-07		intergenic	stmn4l, il17a
4_16319893	4	16319893	C/A	0.221	0.0254	5.1E-07	1.41E-06		intron	itpr2
7_13569992	7	13569992	C/T	0.054	0.0216	3.49E-06	3.76E-06		5'UTR	med19a
7_13642433	7	13642433	G/A	0.059	0.0282	1.16E-07*	1.15E-07*		intron	znf8l
7_14517232	7	14517232	A/T	0.054	0.0249	6.41E-07	1.25E-06		intergenic	pcdh2ac
7_21186138	7	21186138	C/T	0.052	0.0247	7.02E-07	1.3E-06		intergenic	nrg2b
13_8265662	13	8265662	T/C	0.098	0.0273	1.86E-07	4.99E-07		missense	skila
13_9173867	13	9173867	A/G	0.103	0.0222	2.64E-06	2.94E-06		synonymous	pde1c
13_9399249	13	9399249	T/C	0.092	0.0294	6.28E-08*	1.79E-07*		intergenic	vwc2l
13_11658911	13	11658911	C/T	0.103	0.0233	1.45E-06	1.75E-06		intron	phlpp1
13_11658913	13	11658913	G/T	0.103	0.0233	1.45E-06	1.75E-06		intron	
13_11797268	13	11797268	T/C	0.092	0.0244	8.15E-07	2.01E-06		intergenic	igfbp3
13_19862489	13	19862489	A/C	0.106	0.0218	3.14E-06	4.35E-06		intron	mmp14
17_9912197	17	9912197	A/G	0.101	0.0249	6.55E-07	1.13E-06		intergenic	dlx6a
17_21270002	17	21270002	C/G	0.076	0.0210	4.78E-06	1.02E-06		intron	nmda2d
19_5083193	19	5083193	G/A	0.459	0.0238	1.14E-06	1.37E-06		intron	
20_19316641	20	19316641	A/C	0.131	0.0305	3.59E-08*	4.86E-08*		intron	cdh6l
23_3068967	23	3068967	C/G	0.062	0.0230	1.72E-06	3.75E-07		intron	rap1gds1
24_2770096	24	2770096	A/G	0.057	0.0214	3.83E-06	2.57E-06		intron	prkx
24_3585432	24	3585432	A/C	0.056	0.0240	1.02E-06	2.7E-06	9.12E-07	intron	bmpr2l
24_3601736	24	3601736	T/G	0.053	0.0243	8.93E-07*	4.95E-07	9.32E-07	intron	

Allele, minor/major allele. PVE, the phenotypic variance explained of r.U_{crit}. *P*-values exceeded the suggestive threshold are showed of each swimming performance traits: p1, absolute critical swimming speed (a.U_{crit}); p2, relative swimming speed (r.U_{crit}); p3, binary trait (the SS and IS individuals, recorded as 1 and 2, respectively). *, *P*-values exceeded the significant threshold. SS (superior swimmers) and IS (inferior swimmers) were classified by a.U_{crit}. Upstream and downstream interval size is 5 kb.

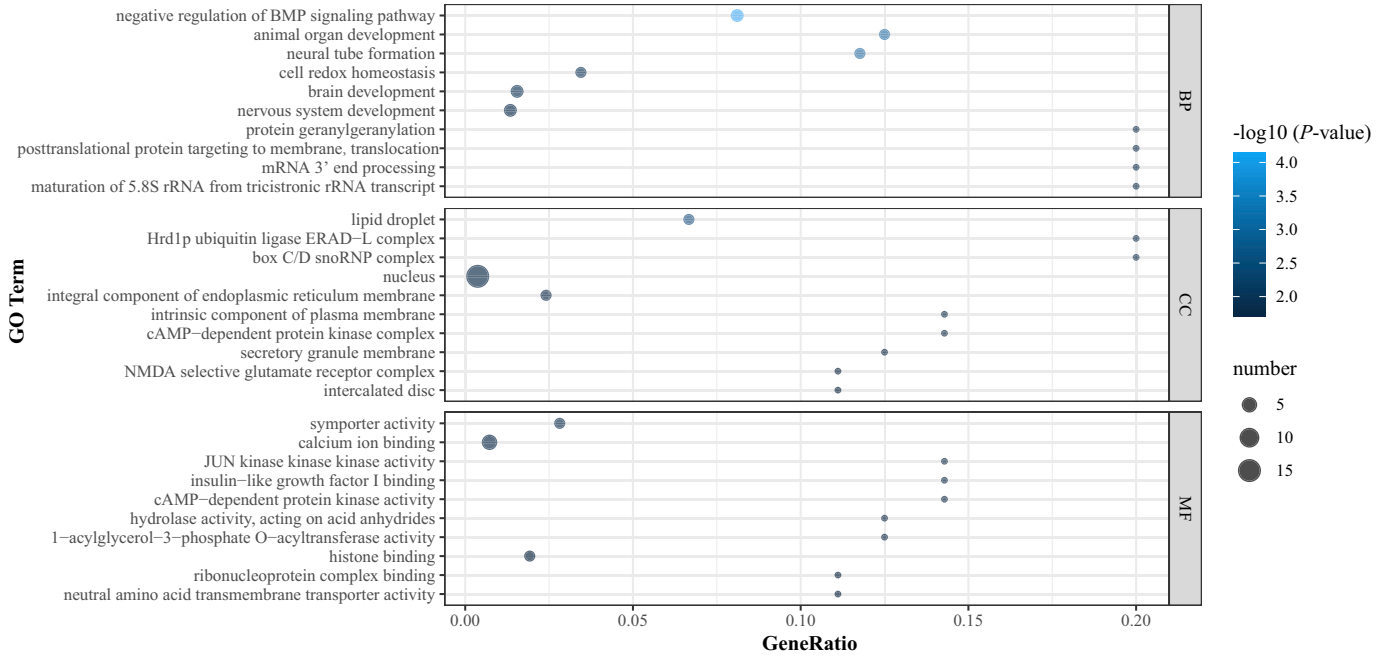

Fig. 7. The top 10 Gene Ontology (GO) terms for three main categories enriched by functional genes annotated around related SNPs. The size and color of bubbles represent the number of candidate genes in each GO terms and -log10 (*P*-value), respectively. The horizontal axis of bubbles show the GeneRatio.

underlying cardiac performance (McKenzie et al., 2021). A more effective strategy would be to integrate multiple phenotypic traits in molecular breeding programs to ensure both performance and robustness.

4.2. *The genetic basis of swimming performance in spotted sea bass*

Despite advancements in understanding fish swimming performance, the genetic basis for this trait remains largely unexplored. 25 loci related to swimming performance traits were obtained through GWAS; however, only 5 of them were significant markers that exceeded the genome-wide significant threshold of 0.05/N, which may due to the relatively small sample size and the polygenetic feature of this trait. A total of 85 candidate genes were annotated by scanning the upstream and downstream regions of these SNPs. Among the five significant SNPs, loci 7_13,642,433, 20_19,316,641 and 24_3,601,736 were located in the intronic regions of zinc finger protein 8-like (*znf8l*), cadherin 6-like

Table 3
Variance components for two continuous swimming performance traits in spotted sea bass.

	$\sigma_g^2 \pm$ S.E.	$\sigma_e^2 \pm$ S.E.	$h^2 \pm$ S.E.
Absolute critical swimming speed (a. U_{crit})	15.53 ± 6.58	58.52 ± 6.24	0.21 ± 0.08
Relative critical swimming speed (r. U_{crit})	0.24 ± 0.10	0.84 ± 0.09	0.22 ± 0.08

σ_g^2, additive genetic variance. σ_e^2,Residual variance. h^2,genomic heritability. S.E., standard error.

(*cdh6l*) and bone morphogenetic protein receptor 2-like (*bmpr2l*), respectively. Z*nf8l* is predicted to act upstream of or within the BMP signaling pathway (Jiao et al., 2002), which plays a vital part in the skeletal and morphological development of teleosts (Ahi, 2016). This suggests that *znf8l* may be a potential gene influencing fish swimming performance. *Cdh6l* plays a role in maintaining tissue integrity and regulating cellular processes such as development, differentiation, and morphogenesis (Jia et al., 2011), suggesting that its = may involve in the skeletal muscle health of spotted sea bass. *Bmpr2l* is likely important for bone health in spotted sea bass, as mutations in *bmpr2* have been associated with bone-related issues that affect physical performance (Sanchez-Duffhues et al., 2020). Furthermore, *bmpr2l* may influence the development of cardiac muscle cells as well (Du et al., 2022), which is critical for swimming performance (Claireaux et al., 2005).

In addition, several genes associated with muscle function were identified. Inositol 1,4,5-trisphosphate receptor, type 2 (*itpr2*) could regulate the releasing of intracellular calcium (Mei et al., 2021), suggesting that it may influence swimming performance by impacting the efficiency and speed of muscle contraction. The phosphatase and actin regulator gene family can bind to actin and regulate the reorganization of the actin cytoskeleton (W. Lin et al., 2022). Thus, phosphatase and actin regulator 1 (*phactr1*) may impact muscle function by regulating the actin cytoskeleton in skeletal muscle cells (Squire, 2019). Moreover, matrix metallopeptidase 14 (*mmp14*) was detected near SNP 13_19,862,489 and may play a crucial role in skeletal muscle repair (Snyman and Niesler, 2015). Although individual variation in swimming performance has been linked to muscle biochemistry (Kolok, 1992; Martinez et al., 2002), swimming performance hierarchies remained consistent despite changes in muscle metabolic level, indicating that muscle metabolism is not the dominance for individual swimming ability (Martinez et al., 2002).

Several genes related to lipid and energy metabolism were also annotated. Lipid storage in adipose tissue is crucial for energy homeostasis, genes such as lysophosphatidylcholine acyltransferase 2 (*lpcat2*), solute carrier family 43 member 1a (*slc43a3b*), NAD kinase b (*nadkb*), and meprin A (*mep1b*) have been reported to play roles in lipid metabolism, potentially contributing to the maintenance of intracellular lipid balance and energy metabolism (Gooding et al., 2019; Hasbargen et al., 2020; Y. H. Lin et al., 2024; Xu et al., 2021). Cardiotrophin-like cytokine factor 1 (*clcf1*) signaling has been reported to impair thermogenesis and disrupt metabolic homeostasis by inhibiting mitochondrial biogenesis in brown adipocytes (M. Ding et al., 2023; Yuan et al., 2024), while RAP1, GTP-GDP dissociation stimulator 1 (*rap1gds1*) regulates mitochondrial dynamics by controlling RHOT function to promote mitochondrial fission under high calcium conditions (L. G. Ding et al., 2016). These findings suggest that these genes may influence fish swimming performance by modulating mitochondrial activity. The upregulation of PH domain and leucine rich repeat protein phosphatase 1 (*phlpp1*) has been associated with obesity and type 2 diabetes due to its interference with Akt-mediated insulin signaling (Lupse et al., 2022). Therefore, it is anticipated that *phlpp4* may affect swimming performance by

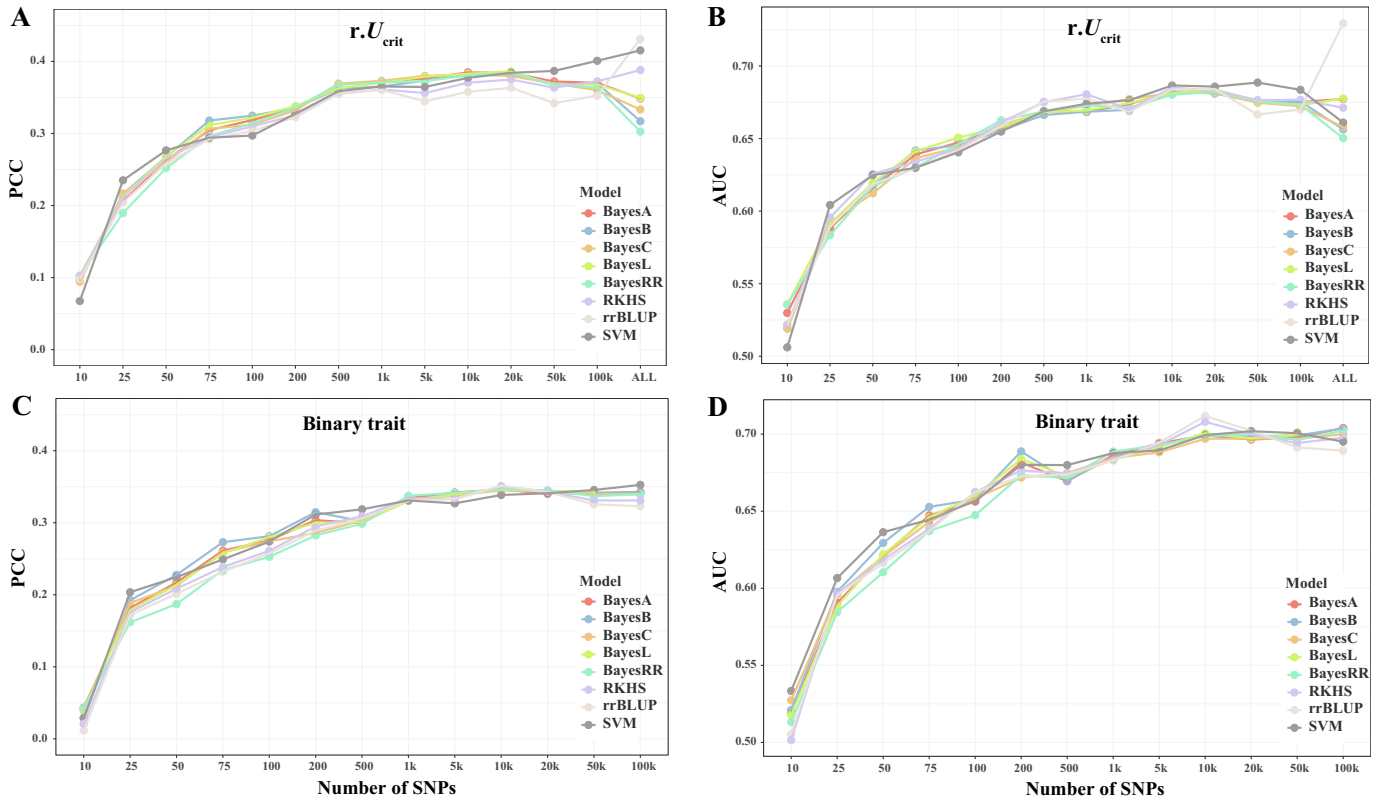

Fig. 8. Comparison of prediction accuracies of eight different models for continuous trait and binary trait of swimming performance. (A) and (C) The prediction accuracy evaluated by Pearson correlation coefficient (PCC) between the observed phenotypes and GEBV of testing population using different models for relative swimming speed (r.U_{crit}) and binary trait (i.e., IS and SS), respectively. (B) and (D) The AUC (area under the curve) using different models for r.U_{crit} and binary trait, respectively.

participating in glucose and lipid metabolism.

Genes associated with the nervous system were also annotated: distal-less homeobox 6a (*dlx6a*), neuronal differentiation 6b (*neurod6b*), von Willebrand factor C domain containing 2-like (*vwc2l*), stathmin-like 4 (*stmn4l*), membrane progestin receptor beta-like (*paqr8l*), and adenylate cyclase type 1-like (*adcy1l*) are involved in the development and maintenance of the nervous system (Cobos et al., 2005; Kasubuchi et al., 2017; M. J. Lin and Lee, 2016; Miwa et al., 2009; Tutukova et al., 2021; Xia et al., 1993), which is vital for motor abilities. Additionally, solute carrier family 1 member 1 (*slc1a1*) is involved in the uptake of glutamate, a major excitatory neurotransmitters in the central nervous system (Bailey et al., 2011). Solute carrier family 6 member 2 (*slc6a2*) is responsible for the reuptake of extracellular norepinephrine (NE) into presynaptic nerve terminals, and a rare variant of *slc6a2* has been strongly associated with elite athletic performance (Fichna et al., 2021; Guilherme et al., 2019). Therefore, we hypothesize that *slc6a2* could also play a significant role in individual swimming performance in fish. Moreover, neuregulin 2b (*nrg2b*) has been shown to promote neuronal survival and neurite extension in rats (Nakano et al., 2016), suggesting a role in controlling fish locomotion. Glutamate receptor ionotropic (*nmda2d*) plays an important role in long-term adaptive and regulatory processes in the brain (Hallett and Standaert, 2004), which may aid fish in adjusting their swimming strategies.

Previous research has shown that fish with superior swimming performance tend to exhibit higher cardiac power output than poor swimmers (Claireaux et al., 2005). In this study, several genes (desmoplakin a (*dspa*), smoothelin-like (*smtn*) and phosphodiesterase 1C (*pde1c*)) related to the structure and formation of cardiac muscle and vascular smooth muscle cells were detected, which may influence the cardiac function in fish (Boyer et al., 2010; Satoh et al., 2015; Tian et al., 2019). Additionally, several genes were found to affect swimming performance through multiple mechanisms: protein kinase X-linked (*prkx*) could affect blood maturation and neural development (Huang et al., 2016), while insulin-like growth factor-binding protein 1 (*igfbp1*) and insulin-like growth factor-binding protein 3 (*igfbp3*) may elevate the blood glucose levels and influence the biosynthesis of muscle protein (Lang et al., 2003; Lewitt et al., 1991). Matrix metallopeptidase 2 (*mmp2*) is primarily involved in the regulation of stem cell activity that give rise to new granule neurons (Sîrbulescu et al., 2015), and inhibiting *mmp2* can also impact fin regeneration in teleosts, which is a key factor in swimming ability (Rajaram et al., 2016).

Moreover, previous studies have shown that fish with enhanced swimming performance tend to exhibit improved disease resistance (Castro et al., 2011; Castro et al., 2013; Zeng et al., 2023). In line with this, several genes related to disease resistance were also identified: interleukin 17a (*il17a*), zinc finger DHHC-type palmitoyltransferase 5b (*zdhhc5b*) and receptor-interacting protein kinase 1 (*ripk1l*) play significant roles in various immune and inflammatory responses, and are crucial to the host's defense against numerous pathogens (Cho et al., 2009; Iwakura et al., 2008; Lu et al., 2019). These findings further support the correlation between swimming performance and overall robustness.

Based on the current results, we believed that the swimming performance of spotted sea bass was a complex trait, the clarification of genetic architecture of which could be a long and difficult process. Additionally, the candidate genes annotated herein require further investigation to elucidate their roles related to swimming performance of fish. Therefore, more studies are needed to improve the results of the present study.

4.3. The GP for swimming performance in spotted sea bass

The heritability estimates of a.U_{crit} and r.U_{crit} of spotted sea bass were 0.21 ± 0.08 and 0.22 ± 0.08, respectively, indicating that the swimming performance of spotted sea bass is a heritable trait. Similarly, studies on other fish species have identified swimming performance to have moderate to high heritability. For example, the heritability of swimming performance was estimated in Nile tilapia (*Oreochromis niloticus*) (a.U_{crit}: 0.48 ± 0.17, r.U_{crit}: 0.15 ± 0.13) (Mengistu et al., 2021), threespine stickleback (*Gasterosteus aculeatus*) (absolute and relative burst swimming speed: 0.41 and 0.37, respectively) (Garenc et al., 1998), guppy (*Poecilia reticulata*) (a.U_{crit}: 0.25 ± 0.15) (Nicoletto, 1995), large yellow croaker (a.U_{crit}: 0.26 ± 0.05, r.U_{crit}: 0.22 ± 0.09) (Zeng et al., 2022) and European sea bass (*Dicentrarchus labrax*) (maximum burst swimming speed: 0.55 ± 0.08) (Vandeputte et al., 2016). Given that the estimates were derived from SNP analyses, we anticipated that the heritability calculated through family studies on swimming performance in spotted sea bass may yield higher values (López-Cortegano and Caballero, 2019; Manolio et al., 2009). Overall, these results suggested that the feasibility of artificial selection for swimming performance traits in spotted sea bass.

It takes 3–4 years for spotted sea bass to reach sexual maturity (Liu et al., 2020), making the selective breeding of this species a time-consuming and costly endeavor. Consequently, the development of molecular breeding could facilitate the promotion of germplasm of spotted sea bass by reducing the time and effort investments of breeding programs (Fugeray-Scarbel et al., 2021). The evaluation cost and prediction accuracy are somewhat interconnected, as higher spending on the evaluation could improve the accuracy (Fugeray-Scarbel et al., 2021). Despite the current decrease in high-throughput sequencing costs, it remains a significant impediment to the implementation of GS in aquacultural breeding programs (Song and Hu, 2022; Zhang et al., 2023).

To our knowledge, this is the first study to assess genomic predictions for swimming performance traits in spotted sea bass. The accuracy of GP could be influenced by heritability, linkage disequilibrium, population size, genetic architecture of the traits and other factors (Morgante et al., 2018). Therefore, it's essential to compare the performance of different models when analyzing new traits in a species (Barria et al., 2021). In the present study, SNP markers were selected based on the GWAS result to improve the prediction accuracy of GP (Jeong et al., 2020; Nani et al., 2019). PCC and AUC were used to quantify the prediction ability of GP. PCC represents the correlation coefficient between the observed phenotypes and GEBV of testing population (Bian and Holland, 2017; K. Q. Wang et al., 2022), while AUC is a matric that measures how well a model can distinguish positive and negative actuals (Simundic, 2009; K. Q. Wang et al., 2022). Therefore, by using AUC, we could assess which model is more suitable for distinguishing the superior swimmers (SS) from the breeding population. We compared the prediction accuracies of GS models using different SNP densities. With the increasing density of SNPs, the PCC and AUC of different models rose gradually, indicating that sufficient density of SNPs is crucial to the accuracy of prediction (Barria et al., 2021; Yoshida et al., 2019). For the continuous trait of swimming performance, a stable predictive ability (PCC: 0.36, and AUC: 0.67) could be achieved when the number of SNPs reached 500 for all models. In contrast, for the binary trait, a stable prediction ability (PCC: 0.33, and AUC: 0.68) could be gained when the number of SNP markers reached 1000, indicating that predictions for continuous trait could provide more accurate results with a lower SNP density compared to those for binary trait.

The prediction abilities of different models for the binary trait of swimming performance were compared in large yellow croaker, and the prediction accuracies estimated by PCC were nearly the same between GBLUP (0.21 ± 0.08) and BayesB (0.21 ± 0.06) (Zeng et al., 2023). Similarly, the prediction ability among eight various models (rrBLUP, BayesA, BayesB, BayesC, BayesRR, BayesL, RKHS and SVM) resembled in trends with the change of SNP number. However, though the AUC between continuous trait (r.U_{crit}) and binary trait showed no significant difference, a slightly higher PCC was observed when using r.U_{crit}. This indicated that using r.U_{crit} in GP could provide a higher prediction accuracy. Moreover, the comparison of computational time among each model showed that rrBLUP and SVM performed better than other

models, indicating these two models have better prediction efficiency for swimming performance. Notably, SVM showed slightly higher PCC than rrBLUP at low density (500-50 K) of markers. In general, when using relatively low SNP density (500-50 K) to estimate the continuous trait of swimming ability of individuals, we recommend using SVM to calculate GEBV in terms of prediction accuracy and efficiency.

5. Conclusion

Our results demonstrated clear individual differences of swimming performance among spotted sea bass. Through testing the critical swimming speed, individuals in the test population were classified as IS and SS. To investigate the genetic basis of swimming performance, GWAS were conducted for swimming performance of spotted sea bass. A total of 85 candidate genes associated with swimming performance were identified near 25 associated SNPs. GO enrichment analysis indicated that these candidate genes may directly or indirectly regulate swimming performance through multiple biological processes. And the heritability estimates of a.U_{crit} and r.U_{crit} were moderate (0.21 ± 0.08 and 0.22 ± 0.08, respectively). Additionally, GP was performed to compare the prediction accuracy of traditional and machine learning models under different SNP densities. The continuous trait and SVM model were recommended for calculating GEBV, and the suggestive SNP density for prediction was 500. This study established a foundation for further investigation into the genetic mechanisms of swimming performance and provide theoretical support for future selection breeding of new strains of spotted sea bass suited for deeper offshore aquaculture.

Supplementary data to this article can be found online at https://doi.org/10.1016/j.aquaculture.2024.741962.

Funding

This research was funded by National Key Research and Development Program of China [grant number: 2022YFD2400103] and Agriculture Research System of China (CARS for Marine Fish Culture Industry) [grant number: CARS-47].

CRediT authorship contribution statement

Hao Li: Writing – original draft, Visualization, Methodology, Investigation, Formal analysis. **Chong Zhang:** Writing – review & editing, Software, Methodology. **Haishen Wen:** Supervision, Conceptualization. **Xin Qi:** Resources, Conceptualization. **Yani Dong:** Methodology, Investigation. **Cong Liu:** Software, Methodology. **Yonghang Zhang:** Software, Methodology. **Chunxiang Niu:** Investigation. **Yun Li:** Writing – review & editing, Supervision, Funding acquisition, Conceptualization.

Declaration of competing interest

The authors declare that they have no known competing financial interests or personal relationships that could have appeared to influence the work reported in this paper.

Data availability

Data will be made available on request.

Acknowledgement

We would like to thank the lab members who lent a helping hand to this study. And we are grateful for the constructive suggestions given by the reviewers.

References

Ahi, E.P., 2016. Signalling pathways in trophic skeletal development and morphogenesis: insights from studies on teleost fish. Dev. Biol. 420 (1), 11–31. https://doi.org/10.1016/j.ydbio.2016.10.003.

Alexander, D.H., Novembre, J., Lange, K., 2009. Fast model-based estimation of ancestry in unrelated individuals. Genome Res. 19 (9), 1655–1664. https://doi.org/10.1101/gr.094052.109.

Arbeláez-Rojas, G.A., Moraes, G., Nunes, C.D., Fabrizzi, F., 2017. Sustained swimming mitigates stress in juvenile *Brycon amazonicus* reared in high stocking densities. Pesq. Agrop. Brasileira 52 (1), 1–9. https://doi.org/10.1590/S0100-204x2017000100001.

Bailey, C.G., Ryan, R.M., Thoeng, A.D., Ng, C., King, K., Vanslambrouck, J.M., Rasko, J.E. J., 2011. Loss-of-function mutations in the glutamate transporter SLC1A1 cause human dicarboxylic aminoaciduria. J. Clin. Investig. 121 (1), 446–453. https://doi.org/10.1172/Jci44474.

Barria, A., Benzie, J.A.H., Houston, R.D., De Koning, D.J., de Verdal, H., 2021. Genomic selection and genome-wide association study for feed-efficiency traits in a farmed Nile Tilapia (*Oreochromis niloticus*) population. Front. Genet. 12. https://doi.org/10.3389/fgene.2021.737906.

Beamish, F.W.H., 1978. Swimming capacity. In: Hoar, W.S., Randall, J.D. (Eds.), Fish Physiology, vol. 7. Academic Press Inc., New York, pp. 101–187.

Bian, Y., Holland, J.B., 2017. Enhancing genomic prediction with genome-wide association studies in multiparental maize populations. Heredity 118 (6), 585–593. https://doi.org/10.1038/hdy.2017.4.

Boyer, J.G., Bernstein, M.A., Boudreau-Larivière, C., 2010. Plakins in striated muscle. Muscle Nerve 41 (3), 299–308. https://doi.org/10.1002/mus.21472.

Brett, 1964. The Respiratory Metabolism and Swimming Performance of Young Sockeye Salmon..

Cano-Barbacil, C., Radinger, J., Argudo, M., Rubio-Gracia, F., Vila-Gispert, A., Garcia-Berthou, E., 2020. Key factors explaining critical swimming speed in freshwater fish: a review and statistical analysis for Iberian species. Sci. Rep. 10 (1). https://doi.org/10.1038/s41598-020-75974-x.

Castro, V., Grisdale-Helland, B., Helland, S.J., Kristensen, T., Jorgensen, S.M., Helgerud, J., Takle, H., 2011. Aerobic training stimulates growth and promotes disease resistance in Atlantic salmon (*Salmo salar*). Comp. Biochem. Physiol. A Mol. Integr. Physiol. 160 (2), 278–290. https://doi.org/10.1016/j.cbpa.2011.06.013.

Castro, V., Grisdale-Helland, B., Jorgensen, S.M., Helgerud, J., Claireaux, G., Farrell, A. P., Takle, H., 2013. Disease resistance is related to inherent swimming performance in Atlantic salmon. BMC Physiol. 13, 1. https://doi.org/10.1186/1472-6793-13-1.

Chen, Y.X., Chen, Y.S., Shi, C.M., Huang, Z.B., Zhang, Y., Li, S.K., Chen, Q., 2017. SOAPnuke: a MapReduce acceleration-supported software for integrated quality control and preprocessing of high-throughput sequencing data. Gigascience 7 (1). https://doi.org/10.1093/gigascience/gix120.

Cho, Y., Challa, S., Moquin, D., Genga, R., Ray, T.D., Guildford, M., Chan, F.K.M., 2009. Phosphorylation-driven assembly of the RIP1-RIP3 complex regulates programmed necrosis and virus-induced inflammation. Cell 137 (6), 1112–1123. https://doi.org/10.1016/j.cell.2009.05.037.

Cingolani, P., Platts, A., Wang, L.L., Coon, M., Nguyen, T., Wang, L., Ruden, D.M., 2012. A program for annotating and predicting the effects of single nucleotide polymorphisms, SnpEff: SNPs in the genome of *Drosophila melanogaster* strain w1118; iso-2. Fly 6 (2), 80–92. https://doi.org/10.4161/fly.19695.

Claireaux, G., McKenzie, D.J., Genge, A.G., Chatelier, A., Aubin, J., Farrell, A.P., 2005. Linking swimming performance, cardiac pumping ability and cardiac anatomy in rainbow trout. J. Exp. Biol. 208 (Pt 10), 1775–1784. https://doi.org/10.1242/jeb.01587.

Cobos, I., Broccoli, V., Rubenstein, J.L.R., 2005. The vertebrate ortholog of Aristaless is regulated by Dlx genes in the developing forebrain. J. Comp. Neurol. 483 (3), 292–303. https://doi.org/10.1002/cne.20405.

Ding, L.G., Lei, Y., Han, Y.P., Li, Y.H., Ji, X.M., Liu, L., 2016. Vimar is a novel regulator of mitochondrial fission through Miro. PLoS Genet. 12 (10). https://doi.org/10.1371/journal.pgen.1006359.

Ding, M., Xu, H.Y., Zhou, W.Y., Xia, Y.F., Li, B.Y., Shi, Y.J., Tang, Q.Q., 2023. CLCF1 signaling restrains thermogenesis and disrupts metabolic homeostasis by inhibiting mitochondrial biogenesis in brown adipocytes. Proc. Natl. Acad. Sci. U. S. A. 120 (33). https://doi.org/10.1073/pnas.2305717120.

Drucker, E.G., 1996. The use of gait transition speed in comparative studies of fish locomotion. Am. Zool. 36 (6), 555–566.

Du, M.X., Jiang, H.B., Liu, H.X., Zhao, X., Zhou, Y., Zhou, F., Yang, J., 2022. Single-cell RNA sequencing reveals that BMPR2 mutation regulates right ventricular function via ID genes. Eur. Respir. J. 60 (1). https://doi.org/10.1183/13993003.00327-2021.

Endelman, J.B., 2011. Ridge regression and other kernels for genomic selection with R package rrBLUP. Plant Genome 4 (3), 250–255. https://doi.org/10.3835/plantgenome2011.08.0024.

Farrell, A.P., 2008. Comparisons of swimming performance in rainbow trout using constant acceleration and critical swimming speed tests. J. Fish Biol. 72 (3), 693–710. https://doi.org/10.1111/j.1095-8649.2007.01759.x.

Fichna, J.P., Huminska-Lisowska, K., Safranow, K., Adamczyk, J.G., Cieszczyk, P., Zekanowski, C., Berdynski, M., 2021. Rare variant in the SLC6A2 encoding a norepinephrine transporter is associated with elite athletic performance in the polish population. Genes 12 (6). https://doi.org/10.3390/genes12060919.

Fugeray-Scarbel, A., Bastien, C., Dupont-Nivet, M., Lemarié, S., Consortium, R.D., 2021. Why and how to switch to genomic selection: lessons from plant and animal breeding experience. Front. Genet. 12. https://doi.org/10.3389/fgene.2021.629737.

Garenc, C., Silversides, F.G., Guderley, H., 1998. Burst swimming and its enzymatic correlates in the threespine stickleback (*Gasterosteus aculeatus*): full-sib heritabilities. Can. J. Zool. 76 (4), 680–688. https://doi.org/10.1139/cjz-76-4-680.

González-Recio, O., Rosa, G.J.M., Gianola, D., 2014. Machine learning methods and predictive ability metrics for genome-wide prediction of complex traits. Livest. Sci. 166, 217–231. https://doi.org/10.1016/j.livsci.2014.05.036.
Gooding, J., Cao, L., Whitaker, C., Mwiza, J.M., Fernander, M., Ahmed, F., Ongeri, E.M., 2019. Meprin metalloproteases associated with differential metabolite profiles in the plasma and urine of mice with type 1 diabetes and diabetic nephropathy. BMC Nephrol. 20. https://doi.org/10.1186/s12882-019-1313-2.
Gregory, T.R., Wood, C.M., 1998. Individual variation and interrelationships between swimming performance, growth rate, and feeding in juvenile rainbow trout (*Oncorhynchus mykiss*). Can. J. Fish. Aquat. Sci. 55 (7), 1583–1590. https://doi.org/10.1139/cjfas-55-7-1583.
Grimmelpont, M., Milinkovitch, T., Dubillot, E., Lefrancois, C., 2022. Individual aerobic performance and anaerobic compensation in a temperate fish during a simulated marine heatwave. Sci. Total Environ. 160844. https://doi.org/10.1016/j.scitotenv.2022.160844.
Guilherme, J.P.L.F., Bigliassi, M., Lancha, A.H., 2019. Association study of SLC6A2 gene Thr99Ile variant (rs1805065) with athletic status in the Brazilian population. Gene 707, 53–57. https://doi.org/10.1016/j.gene.2019.05.013.
Hallett, P.J., Standaert, D.G., 2004. Rationale for and use of NMDA receptor antagonists in Parkinson's disease. Pharmacol. Ther. 102 (2), 155–174. https://doi.org/10.1016/j.pharmthera.2004.04.001.
Handelsman, C., Claireaux, G., Nelson, J.A., 2010. Swimming ability and ecological performance of cultured and wild European sea bass (*Dicentrarchus labrax*) in coastal tidal ponds. Physiol. Biochem. Zool. 83 (3), 435–445. https://doi.org/10.1086/651099.
Hanson, K.C., Hasler, C.T., Suski, C.D., Cooke, S.J., 2007. Morphological correlates of swimming activity in wild largemouth bass (*Micropterus salmoides*) in their natural environment. Comp. Biochem. Physiol. A Mol. Integr. Physiol. 148 (4), 913–920. https://doi.org/10.1016/j.cbpa.2007.09.013.
Hasbargen, K.B., Shen, W.J., Zhang, Y.Q., Hou, X.M., Wang, W., Shuo, Q., Kraemer, F.B., 2020. Slc43a3 is a regulator of free fatty acid flux. J. Lipid Res. 61 (5), 734–745. https://doi.org/10.1194/jlr.RA119000294.
Howard, R., Carriquiry, A.L., Beavis, W.D., 2014. Parametric and nonparametric statistical methods for genomic selection of traits with additive and epistatic genetic architectures. G3-Genes Genom. Genet. 4 (6), 1027–1046. https://doi.org/10.1534/g3.114.010298.
Huang, S.Z., Li, Q., Alberts, I., Li, X.H., 2016. PRKX, a novel cAMP-dependent protein kinase member, plays an important role in development. J. Cell. Biochem. 117 (3), 566–573. https://doi.org/10.1002/jcb.25304.
Iwakura, Y., Nakae, S., Saijo, S., Ishigame, H., 2008. The roles of IL-17A in inflammatory immune responses and host defense against pathogens. Immunol. Rev. 226, 57–79. https://doi.org/10.1111/j.1600-065X.2008.00699.x.
Jain, K.E., Hamilton, J.C., Farrell, A.P., 1997. Use of a ramp velocity test to measure critical swimming speed in rainbow trout (*Onchorhynchus mykiss*). Comp. Biochem. Physiol. A Physiol. 117 (4), 441–444. https://doi.org/10.1016/s0300-9629(96)00234-4.
Jeong, S., Kim, J.Y., Kim, N., 2020. GMStool: GWAS-based marker selection tool for genomic prediction from genomic data. Sci. Rep. 10 (1). https://doi.org/10.1038/s41598-020-76759-y.
Jia, L.W., Liu, F.M., Hansen, S.H., ter Beest, M.B.A., Zegers, M.M.P., 2011. Distinct roles of cadherin-6 and E-cadherin in tubulogenesis and lumen formation. Mol. Biol. Cell 22 (12), 2031–2041. https://doi.org/10.1091/mbc.E11-01-0038.
Jiao, K., Zhou, Y.N., Hogan, B.L.M., 2002. Identification of mZnf8, a mouse kruppel-like transcriptional repressor, as a novel nuclear interaction partner of smad1. Mol. Cell. Biol. 22 (21), 7633–7644. https://doi.org/10.1128/mcb.22.21.7633-7644.2002.
Jing, A.G., Zhang, X.M., Li, W.T., 2005. A preliminary experiment on the swimming ability of Latedabrax maculatus and Sebastes schlegeli. Period. Ocean Univ. China 35 (06), 95–98. https://doi.org/10.16441/j.cnki.hdxb.2005.06.017.
Karatzoglou, A., Smola, A., Hornik, K., Zeileis, A., 2004. kernlab - An S4 Package for Kernel Methods in R. - 11(− 9). https://doi.org/10.18637/jss.v011.i09.
Kasubuchi, M., Watanabe, K., Hirano, K., Inoue, D., Li, X., Terasawa, K., Kimura, I., 2017. Membrane progesterone receptor beta (mPRβ/Paqr8) promotes progesterone-dependent neurite outgrowth in PC12 neuronal cells via non-G protein-coupled receptor (GPCR) signaling. Sci. Rep. 7. https://doi.org/10.1038/s41598-017-05423-9.
Katopodis, C., Cai, L., Johnson, D., 2019. Sturgeon survival: the role of swimming performance and fish passage research. Fish. Res. 212, 162–171. https://doi.org/10.1016/j.fishres.2018.12.027.
Kern, P., Cramp, R.L., Gordos, M.A., Watson, J.R., Franklin, C.E., 2018. Measuring U(crit) and endurance: equipment choice influences estimates of fish swimming performance. J. Fish Biol. 92 (1), 237–247. https://doi.org/10.1111/jfb.13514.
Kolok, A.S., 1992. Morphological and physiological correlates with swimming performance in juvenile largemouth bass. Am. J. Phys. 263 (5), R1042–R1048. https://doi.org/10.1152/ajpregu.1992.263.5.R1042.
Kolok, A.S., 2001. Sublethal identification of susceptible individuals: using swim performance to identify susceptible fish while keeping them alive. Ecotoxicology 10 (4), 205–209. https://doi.org/10.1023/a:1016613209877.
Kolok, A.S., Farrell, A.P., 1994. Individual variation in the swimming performance and cardiac-performance of northern squawfish, *Ptychocheilus-oregonensis*. Physiol. Zool. 67 (3), 706–722. https://doi.org/10.1086/physzool.67.3.30163766.
Lang, C.H., Vary, T.C., Frost, R.A., 2003. Acute in vivo elevation of insulin-like growth factor (IGF) binding protein-1 decreases plasma free IGF-I and muscle protein synthesis. Endocrinology 144 (9), 3922–3933. https://doi.org/10.1210/en.2002-0192.
Lewitt, M.S., Denyer, G.S., Cooney, G.J., Baxter, R.C., 1991. Insulin-like growth factor-binding protein-1 modulates blood-glucose levels. Endocrinology 129 (4), 2254–2256. https://doi.org/10.1210/endo-129-4-2254.
Li, J., Liu, H., Xiao, Z., Wei, X., Liu, Z., Zhang, Z., 2023. Swimming performance of *Cyprinus carpio* (carp) in China. Heliyon 9 (6), e17014. https://doi.org/10.1016/j.heliyon.2023.e17014.
Lin, M.J., Lee, S.J., 2016. Stathmin-like 4 is critical for the maintenance of neural progenitor cells in dorsal midbrain of zebrafish larvae. Sci. Rep. 6. https://doi.org/10.1038/srep36188.
Lin, W., Chen, Z.P., Mo, X.Y., Zhao, S.L., Wen, Z.X., Cheung, W.H., Chen, B.L., 2022. Phactr1 negatively regulates bone mass by inhibiting osteogenesis and promoting adipogenesis of BMSCs via RhoA/ROCK2. J. Mol. Histol. 53 (1), 119–131. https://doi.org/10.1007/s10735-021-10031-z.
Lin, Y.H., Zhang, X., Wang, Y.H., Yao, W., 2024. LPCAT2-mediated lipid droplet production supports pancreatic cancer chemoresistance and cell motility. Int. Immunopharmacol. 139. https://doi.org/10.1016/j.intimp.2024.112681.
Liu, Y., Wang, H.L., Wen, H.S., Shi, Y., Zhang, M.Z., Qi, X., Li, Y., 2020. First high-density linkage map and QTL fine mapping for growth-related traits of spotted sea bass (*Lateolabrax maculatus*). Mar. Biotechnol. 22 (4), 526–538. https://doi.org/10.1007/s10126-020-09973-4.
López-Cortegano, E., Caballero, A., 2019. Inferring the nature of missing heritability in human traits using data from the GWAS catalog. Genetics 212 (3), 891–904. https://doi.org/10.1534/genetics.119.302077.
Lu, Y., Zheng, Y.P., Coyaud, E., Zhang, C., Selvabaskaran, A., Yu, Y.Y., Neculai, D., 2019. Palmitoylation of NOD1 and NOD2 is required for bacterial sensing. Science 366 (6464), 460–+. https://doi.org/10.1126/science.aau6391.
Lupse, B., Heise, N., Maedler, K., Ardestani, A., 2022. PHLPP1 deletion restores pancreatic β-cell survival and normoglycemia in the db/db mouse model of obesity-associated diabetes. Cell Death Dis. 8 (1). https://doi.org/10.1038/s41420-022-00853-5.
Mai, K.S., 2021. Exploring the Road to High-Quality Development of Deep-Sea Farming in China. Ocean University of China News. Retrieved from. http://ouceducnxiaobao.ihwrm.com/index/article/articleinfo.html?doc_id=3659710.
Mai, K.S., Xu, H., Xue, C.H., Gu, W.D., Zhang, W.B., Li, Z.J., Yu, B., 2016. Study on strategies for developing offshore as the new spaces for mariculture in China. Strategi. Study CAE 18 (3), 90–95.
Manolio, T.A., Collins, F.S., Cox, N.J., Goldstein, D.B., Hindorff, L.A., Hunter, D.J., Visscher, P.M., 2009. Finding the missing heritability of complex diseases. Nature 461 (7265), 747–753. https://doi.org/10.1038/nature08494.
Martinez, M., Guderley, H., Nelson, J.A., Webber, D., Dutil, J.D., 2002. Once a fast cod, always a fast cod: maintenance of performance hierarchies despite changing food availability in cod (*Gadus morhua*). Physiol. Biochem. Zool. 75 (1), 90–100. https://doi.org/10.1086/339213.
McKenzie, D.J., Hoglund, E., Dupont-Prinet, A., Larsen, B.K., Skov, P.V., Pedersen, P.B., Jokumsen, A., 2012. Effects of stocking density and sustained aerobic exercise on growth, energetics and welfare of rainbow trout. Aquaculture 338, 216–222. https://doi.org/10.1016/j.aquaculture.2012.01.020.
McKenzie, D.J., Palstra, A.P., Planas, J., MacKenzie, S., Begout, M.L., Thorarensen, H., Skov, P.V., 2021. Aerobic swimming in intensive finfish aquaculture: applications for production, mitigation and selection. Rev. Aquac. 13 (1), 138–155. https://doi.org/10.1111/raq.12467.
Mei, R.Y., Huang, L.Y., Wu, M.Y., Jiang, C.X., Yang, A.F., Tao, H.P., Qiu, M.S., 2021. Evidence that ITPR2-mediated intracellular calcium release in oligodendrocytes regulates the development of carbonic anhydrase II plus type I/II oligodendrocytes and the sizes of myelin fibers. Front. Cell. Neurosci. 15. https://doi.org/10.3389/fncel.2021.751439.
Mengistu, S.B., Palstra, A.P., Mulder, H.A., Benzie, J.A.H., Trinh, T.Q., Roozeboom, C., Komen, H., 2021. Heritable variation in swimming performance in Nile tilapia (*Oreochromis niloticus*) and negative genetic correlations with growth and harvest weight. Sci. Rep. 11 (1). https://doi.org/10.1038/s41598-021-90418-w.
Miwa, H., Miyake, A., Kouta, Y., Shimada, A., Yamashita, Y., Nakayama, Y., Itoh, N., 2009. A novel neural-specific BMP antagonist, Brorin-like, of the Chordin family. FEBS Lett. 583 (22), 3643–3648. https://doi.org/10.1016/j.febslet.2009.10.044.
MOA, 2024. China Fisheries Statistical Yearbook 2024. Ministry of Agriculture, China.
Morgante, F., Huang, W., Maltecca, C., Mackay, T.F.C., 2018. Effect of genetic architecture on the prediction accuracy of quantitative traits in samples of unrelated individuals. Heredity 120 (6), 500–514. https://doi.org/10.1038/s41437-017-0043-0.
Nakano, N., Kanekiyo, K., Nakagawa, T., Asahi, M., Ide, C., 2016. NTAK/neuregulin-2 secreted by astrocytes promotes survival and neurite outgrowth of neurons via ErbB3. Neurosci. Lett. 622, 88–94. https://doi.org/10.1016/j.neulet.2016.04.050.
Nani, J.P., Rezende, F.M., Peñagaricano, F., 2019. Predicting male fertility in dairy cattle using markers with large effect and functional annotation data. BMC Genomics 20. https://doi.org/10.1186/s12864-019-5644-y.
Nayeri, S., Sargolzaei, M., Tulpan, D., 2019. A review of traditional and machine learning methods applied to animal breeding. Anim. Health Res. Rev. 20 (1), 31–46. https://doi.org/10.1017/S1466252319000148.
Nicoletto, P.F., 1995. OVspring quality and female choice in the guppy, *Poecilia reticulata*. Anim. Behav. 49 (2), 377–387. https://doi.org/10.1006/anbe.1995.0050.
Norin, T., Clark, T.D., 2016. Measurement and relevance of maximum metabolic rate in fishes. J. Fish Biol. 88 (1), 122–151. https://doi.org/10.1111/jfb.12796.
Oufiero, C.E., Walsh, M.R., Reznick, D.N., Garland Jr., T., 2011. Swimming performance trade-offs across a gradient in community composition in Trinidadian killifish (*Rivulus hartii*). Ecology 92 (1), 170–179. https://doi.org/10.1890/09-1912.1.
Palstra, A.P., Kals, J., Bohm, T., Bastiaansen, J.W.M., Komen, H., 2020. Swimming performance and oxygen consumption as non-lethal indicators of production traits in

Atlantic Salmon and Gilthead seabream. Front. Physiol. 11, 759. https://doi.org/10.3389/fphys.2020.00759.
Pang, X., Fu, S.J., Zhang, Y.G., 2015. Individual variation in metabolism and swimming performance in juvenile black carp (*Mylopharyngodon piceus*) and the effects of hypoxia. Mar. Freshw. Behav. Physiol. 48 (6), 431–443. https://doi.org/10.1080/10236244.2015.1090205.
Pang, X., Pu, D.Y., Xia, D.Y., Liu, X.H., Ding, S.H., Li, Y., Fu, S.J., 2021. Individual variation in metabolic rate, locomotion capacity and hypoxia tolerance and their relationships in juveniles of three freshwater fish species. J. Comp. Physiol. B. 191 (4), 755–764. https://doi.org/10.1007/s00360-021-01382-w.
Peng, D., Zhu, Y., Chu, J., 2023. Strengthen management of offshore aquaculture. Science 381 (6661). https://doi.org/10.1126/science.adj4352.
Perez, P., de los Campos, G., 2014. Genome-wide regression and prediction with the BGLR statistical package. Genetics 198 (2), 483–U463. https://doi.org/10.1534/genetics.114.164442.
Plaut, I., 2000. Resting metabolic rate, critical swimming speed, and routine activity of the euryhaline cyprinodontid, *Aphanius dispar*, acclimated to a wide range of salinities. Physiol. Biochem. Zool. 73 (5), 590–596. https://doi.org/10.1086/317746.
Plaut, I., 2001. Critical swimming speed: its ecological relevance. Comp. Biochem. Physiol. A Mol. Integr. Physiol. 131 (1), 41–50. https://doi.org/10.1016/s1095-6433(01)00462-7.
Rajaram, S., Murawala, H., Buch, P., Patel, S., Balakrishnan, S., 2016. Inhibition of BMP signaling reduces MMP-2 and MMP-9 expression and obstructs wound healing in regenerating fin of teleost fish. Fish Physiol. Biochem. 42 (2), 787–794. https://doi.org/10.1007/s10695-015-0175-1.
Rao, C., Cao, X., Li, L., Zhou, J., Sun, D., Li, B., Chen, J., 2022. Bisphenol AF induces multiple behavioral and biochemical changes in zebrafish (*Danio rerio*) at different life stages. Aquat. Toxicol. 253, 106345. https://doi.org/10.1016/j.aquatox.2022.106345.
Sanchez-Duffhues, G., Williams, E., Goumans, M.J., Heldin, C.H., ten Dijke, P., 2020. Bone morphogenetic protein receptors: structure, function and targeting by selective small molecule kinase inhibitors. Bone 138. https://doi.org/10.1016/j.bone.2020.115472.
Satoh, K., Kikuchi, N., Kurosawa, R., Shimokawa, H., 2015. PDE1C negatively regulates growth factor receptor degradation and promotes VSMC proliferation. Circ. Res. 116 (7), 1098–1100. https://doi.org/10.1161/Circresaha.115.306139.
Shadwick, R.E., Goldbogen, J.A., 2012. Muscle function and swimming in sharks. J. Fish Biol. 80 (5), 1904–1939. https://doi.org/10.1111/j.1095-8649.2012.03266.x.
Shi, J.G., Yu, W.W., Lu, B.C., Cheng, S.Q., 2021. Development status and prospect of Chinese deep-sea cage. J. Fish. China 45 (6), 992–1005. https://doi.org/10.11964/jfc.20200612314.
Shim, H., Chasman, D.I., Smith, J.D., Mora, S., Ridker, P.M., Nickerson, D.A., Stephens, M., 2015. A multivariate genome-wide association analysis of 10 LDL subfractions, and their response to statin treatment, in 1868 Caucasians. PLoS One 10 (4). https://doi.org/10.1371/journal.pone.0120758.
Simundic, A.-M., 2009. Measures of diagnostic accuracy: basic definitions. Ejifcc 19 (4), 203–211.
Sîrbulescu, R.F., Ilies, I., Zupanc, G.K.H., 2015. Matrix metalloproteinase-2 and-9 in the cerebellum of teleost fish: functional implications for adult neurogenesis. Mol. Cell. Neurosci. 68, 9–23. https://doi.org/10.1016/j.mcn.2015.03.015.
Snyman, C., Niesler, C.U., 2015. MMP-14 in skeletal muscle repair. J. Muscle Res. Cell Motil. 36 (3), 215–225. https://doi.org/10.1007/s10974-015-9414-4.
Song, H.L., Hu, H.X., 2022. Strategies to improve the accuracy and reduce costs of genomic prediction in aquaculture species. Evol. Appl. 15 (4), 578–590. https://doi.org/10.1111/eva.13262.
Squire, J., 2019. Special issue: the actin-myosin interaction in muscle: background and overview. Int. J. Mol. Sci. 20 (22). https://doi.org/10.3390/ijms20225715.
Tan, J., Li, H., Guo, W., Tan, H., Ke, S., Wang, J., Shi, X., 2021. Swimming performance of four carps on the Yangtze River for fish passage design. Sustainability 13 (3). https://doi.org/10.3390/su13031575.
Tian, B., Ding, X., Song, Y., Chen, W., Liang, J., Yang, L., Zhou, Y., 2019. Matrix stiffness regulates SMC functions via TGF-β signaling pathway. Biomaterials 221. https://doi.org/10.1016/j.biomaterials.2019.119407.
Tutukova, S., Tarabykin, V., Hernandez-Miranda, L.R., 2021. The role of Neurod genes in brain development, function, and disease. Front. Mol. Neurosci. 14. https://doi.org/10.3389/fnmol.2021.662774.
Van der Auwera, G., O'Connor, B., 2020. Genomics in the cloud: Using Docker. In: GATK, and WDL in Terra, 1st ed. O'Reilly Media.
Vandeputte, M., Porte, J.D., Auperin, B., Dupont-Nivet, M., Vergnet, A., Valotaire, C., Chatain, B., 2016. Quantitative genetic variation for post-stress cortisol and swimming performance in growth-selected and control populations of European sea bass (*Dicentrarchus labrax*). Aquaculture 455, 1–7. https://doi.org/10.1016/j.aquaculture.2016.01.003.
Wang, P., Gui, F., Wu, C., 2010. Swimming ability of *Sciaenops ocellatus*, *Lateolabrax maculatus* and hapalogenys nitens. Oceanol. Limnol. Sin. 41 (6), 923–929.
Wang, K.Q., Yang, B., Li, Q., Liu, S.K., 2022. Systematic evaluation of genomic prediction algorithms for genomic prediction and breeding of aquatic animals. Genes 13 (12). https://doi.org/10.3390/genes13122247.
Wen, H.S., Zhang, M.Z., Li, J., He, F., Li, Y., 2016. Research progress of aquaculture industry and its seed engineering in spotted sea bass (*Lateolabrax maculatus*) of China. Fish. Inf. Strat. 31 (2), 105–111. https://doi.org/10.13233/j.cnki.fishis.2016.02.005.
Xia, Z.G., Choi, E.J., Fan, W., Blazynski, C., Storm, D.R., 1993. Type-I calmodulin-sensitive adenylyl cyclase is neural specific. J. Neurochem. 60 (1), 305–311. https://doi.org/10.1111/j.1471-4159.1993.tb05852.x.
Xu, M.Y., Ding, L., Liang, J.J., Yang, X., Liu, Y., Wang, Y.C., Huang, X., 2021. NAD kinase sustains lipogenesis and mitochondrial metabolismthrough fatty acid synthesis. Cell Rep. 37 (13). https://doi.org/10.1016/j.celrep.2021.110157.
Yang, J.A., Lee, S.H., Goddard, M.E., Visscher, P.M., 2011. GCTA: a tool for genome-wide complex trait analysis. Am. J. Hum. Genet. 88 (1), 76–82. https://doi.org/10.1016/j.ajhg.2010.11.011.
Yoshida, G.M., Lhorente, J.P., Correa, K., Soto, J., Salas, D., Yáñez, J.M., 2019. Genome-wide association study and cost-efficient genomic predictions for growth and fillet yield in Nile Tilapia (*Oreochromis niloticus*). G3-Genes Genom. Genet. 9 (8), 2597–2607. https://doi.org/10.1534/g3.119.400116.
Young, P.S., Cech, J.J., 1993. Effects of exercise conditioning on stress responses and recovery in cultured and wild Young-of-the-year striped bass, *Morone saxatilis*. Can. J. Fish. Aquat. Sci. 50 (10), 2094–2099. https://doi.org/10.1139/f93-233.
Yuan, Y.W., Li, K.L., Ye, X.R., Wen, S.Y., Zhang, Y.N., Teng, F., Zhang, H.J., 2024. CLCF1 inhibits energy expenditure via suppressing brown fat thermogenesis. Proc. Natl. Acad. Sci. U. S. A. 121 (3). https://doi.org/10.1073/pnas.2310711121.
Zeng, J., Long, F., Wang, J., Zhao, J., Ke, Q., Gong, J., Xu, P., 2022. GWAS reveals heritable individual variations in the inherent swimming performance of juvenile large yellow croaker. Aquaculture 559. https://doi.org/10.1016/j.aquaculture.2022.738419.
Zeng, J., Zhao, J., Wang, J., Bai, Y., Long, F., Deng, Y., Xu, P., 2023. Genetic linkage between swimming performance and disease resistance enables multitrait breeding strategies in large yellow croaker. Agric. Commun. 1 (2). https://doi.org/10.1016/j.agrcom.2023.100019.
Zhang, C., Dong, S.S., Xu, J.Y., He, W.M., Yang, T.L., 2019. PopLDdecay: a fast and effective tool for linkage disequilibrium decay analysis based on variant call format files. Bioinformatics 35 (10), 1786–1788. https://doi.org/10.1093/bioinformatics/bty875.
Zhang, C., Wen, H.S., Zhang, Y.H., Zhang, K.Q., Qi, X., Li, Y., 2023. First genome-wide association study and genomic prediction for growth traits in spotted sea bass using whole-genome resequencing. Aquaculture 566. https://doi.org/10.1016/j.aquaculture.2022.739194.
Zhou, X., Stephens, M., 2012. Genome-wide efficient mixed-model analysis for association studies. Nat. Genet. 44 (7), 821–U136. https://doi.org/10.1038/ng.2310.